Effect of Different Heat Treatment Equipment on the Mechanical Properties of Nitinol Wire

A THESIS SUBMITTED TO THE FACULTY OF THE GRADUATE SCHOOL OF THE UNIVERISTY OF MINNESOTA BY

Karl Kabarowski

IN PARTIAL FULFILLMENT OF THE REQUIREMENTS
FOR THE DEGREE OF
MASTER OF SCIENCE IN MECHANICAL ENGINEERING

Dr. Susan Mantell

December 2020

Copyright Page

ACKNOWLEDGEMENTS

I would firstly like to acknowledge my advisor Prof. Susan Mantell for her guidance and insights throughout the project, as well as detailed review of my final work. Additional thanks to my committee members Dr. Arthur Erdman and Dr. Bruce Hammer for their feedback during my thesis defense. I would also like to acknowledge the University of Minnesota Mechanical Engineering Program, for the opportunity to study and research at this University.

Special thanks to my Nitinol mentors Michael Brenzel, Alex Peterson and Saravana Kumar. My development as an engineer with a strong background in nitinol, specifically in applications in the medical device industry is due in large part to the three of you.

I would like to acknowledge the support provided by Heart Leaflet Technologies (HLT), (Maple Grove, MN). Additionally, parts of this work were carried out by Fort Wayne Metals (Fort Wayne, IN), Innovatech Labs, LLC (Plymouth, MN) and Legend Technical Services (St. Paul, MN).

Lastly, I owe much appreciation to my family for their endless support throughout my studies. Thank you.

ABSTRACT

Nitinol is a nickel-titanium shape memory alloy commonly used in the medical device field for many implanted devices because of its unique properties (shape memory and superelasticity). The purpose of this study is to analyze the mechanical behavior differences between Nitinol wire heat treated in a salt bath and Nitinol wire heat treated in a sand bath. The goal was to determine if one heat treatment method is superior to the other when considering the mechanical properties for the design of a transcatheter aortic valve.

Eighteen test groups of Nitinol wire were evaluated by using two different types of heat treatment equipment and varying heat treatment temperature and heat treatment time. Samples from each test group underwent tensile testing with upper plateau strength, lower plateau strength, residual elongation, ultimate tensile strength and elongation recorded. Reducing delivery forces requires a low UPS (UPS less than 89,888 psi). Low chronic outward force was desired for improved fatigue resistance and to reduction of conduction issues caused by high radial force. Therefore, a low LPS (LPS less than 43,220 psi) is desired. A residual elongation less than 0.10% to limit the permanent deformation from loading and unloading. Higher UTS (212,372 psi) and Elongation (18.0%) are also desired for greater design space of stronger and more ductile wire. The tensile data was used to determine what equipment and process parameters yields superior mechanical performance. Results show that there is a limited process space to reach the desired mechanical properties. Heat treatment equipment showed a statistically significant impact in the lower plateau strength, ultimate tensile strength and residual elongation. Sample groups heat treated in the salt bath were more repeatable than the corresponding sand bath

groups. There was no combination of tested time and temperature that yielded positive results. The salt bath had a limited design space to obtain an optimal process. A heat treatment for a time of 2 minutes and 20 seconds at a temperature of ~515°C in the salt bath is located approximately in the middle of the acceptable area determined by a contour plot. Conducting a range finding study for salt bath heat treatment is recommended to verify the study and potentially expand the processing parameter options.

Table of Contents

List of Figures

List of Tables

1 Introduction

1.1 Introduction

In the process of developing a heat and corrosive resistant alloy for the US Naval labs in 1962, William Buehler discovered a new superelastic shape memory alloy made of approximately 55% nickel and 45% titanium. Buehler prepared for a lab management meeting by bending a thin strip of the material into an accordion shape, intending to flex it repeatedly to demonstrate the Nitinol's fatigue resistance, a biproduct of its superelasticity. However, during the meeting someone applied heat to the strip with a lighter and the bent strip immediate straightened back to its original pre-bent shape with considerable force, demonstrating strong shape memory [1]. The team named the alloy Nitinol using the atomic symbols for nickel and titanium (Ni and Ti, respectively) and NOL from Naval Ordinance Laboratory [2]. Nitinol's superelastic and shape memory properties were studied and integrated into advancing the aerospace industry, followed shortly by the medical device industry. Nitinol provides a larger design space for the next generation of designs. The first medical device to take advantage of the unique properties of Nitinol was orthodontic archwires which required a material that would not lose tension over time [3]. Today, Nitinol can be found in many different medical devices in many medical specialties including cardiovascular, neurovascular, endovascular, orthopedic, and urology. To understand why Nitinol has been so widely adopted by the medical device industry, it is important to understand the unique shape memory and superelastic properties.

1.2 Research Objectives and Approach

The effect of the different heat treatment equipment used in Nitinol processing has been mostly overlooked in literature. Fluidized sand bath, fluidized salt baths and furnaces/ovens are the three most commonly chosen equipment for Nitinol heat treatment processes. Both the sand bath and salt bath use conduction to transfer heat to the Nitinol, as opposed to ovens/furnaces which use convection heat transfer. Fast transitions from cold temperatures (room temperature) to the selected heat treatment temperature and a fast transition from the heat treatment temperature back down to the cold temperature is oftentimes desired for more process and output control, namely the austenite finish transition temperature (A_f). This is commonly analyzed either with a thermocouple logging temperature data during a heat treatment or evaluation of the A_f temperatures.

Despite available literature regarding how Nitinol heat treatment parameters affect the mechanical properties, conducting experiments is still crucial to ensure the desired Nitinol properties are obtained when heat treated. The source of the Nitinol, mandrel material, and mandrel mass are a few factors that can contribute to changes in the Nitinol properties from case to case. Therefore, determining heat treatment parameters is an important step in creating a heat treatment process that imparts the desired characteristics to the Nitinol samples. The most relevant properties of superelastic Nitinol include the large recoverable deformation (function of large elongation at break), low residual deformation, and different critical strength measurements: lower plateau strength (LPS) upper plateau strength (UPS) and ultimate tensile strength (UTS).

The different heat treatments will be investigated to improve the mechanical properties of the HLT Meridian transcatheter aortic valve through Nitinol heat treatment processing. The most relevant mechanical properties (UPS, LPS, UTS, Residual Elongation and Elongation) and the A_f temperature will be the outputs of most interest when evaluating the differences in the heat treatment equipment, time, and temperature settings.

2 Literature Review

2.1 Properties of Nitinol

Nitinol is commonly used due to its mechanical properties and unique combination of strength, fatigue durability, corrosion resistance. Nitinol offers an advantageous mix of polymer and metal deemed “strength of a metal and flexibility of plastics” or “super-spring”. These advantageous phenomena are commonly referred to as shape memory and superelasticity. The shape memory and superelasticity can be optimized via control of the A_f temperature

2.1.1 Shape Memory and Superelasticity

Shape memory is the ability of a material to return to its initial shape when heated after being plastically deformed. Superelasticity is the elastic response to an applied stress caused by a phase transformation. These properties are due to Nitinol’s reversible solid-state phase transformations between the high temperature austenite phase and low temperature martensite phase. At zero strain, the austenite phase atomic structure is called cubic B2 crystal structure and the martensite phase atomic structure is called B19’ crystal structure. Schematic crystallographic models of the two structures are shown in Figure 1.

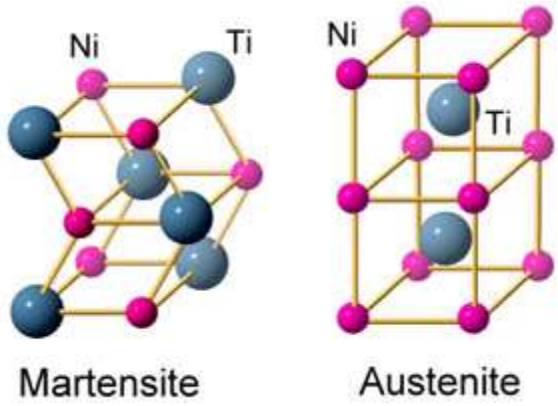

Figure 1: (Left) B19' crystal structure schematic observed in martensite phase under no stress/strain. (Right) B2 crystal structure schematics observed in austenite phase under not stress/strain. [4],[5]

The shape memory effect exhibited by Nitinol not only physically changes the alloy, but also significantly changes the mechanical properties. The modulus of elasticity of Nitinol in the martensite phase is 40GPa. In the austenite phase, the modulus of elasticity is 75GPa. [6]. The combination of shape memory and superelasticity phase transformations contribute to the shape of the stress-strain Nitinol hysteresis at different temperatures (Figure 2).

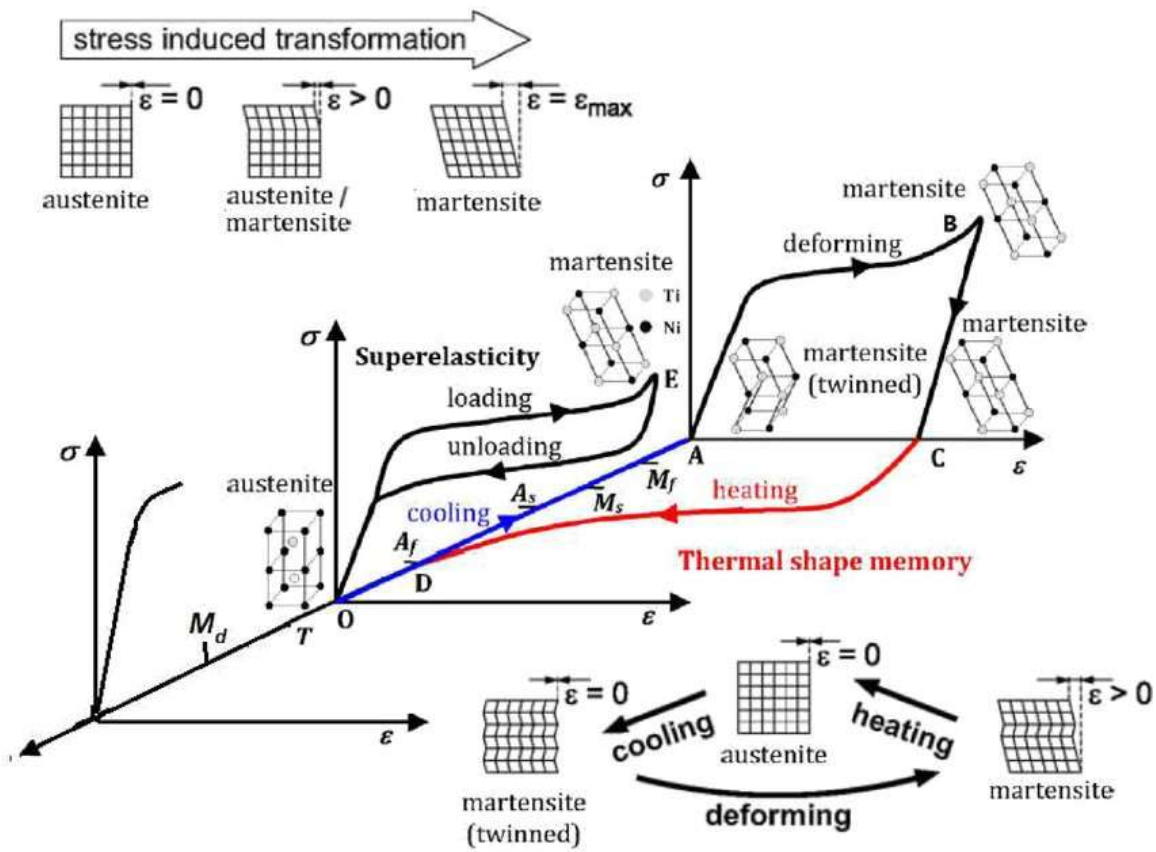

Figure 2: Shape Memory and Superelasticity Nitinol Hysteresis [7]

Starting at point A on the graph in Figure 2, the Nitinol is in an environment with a temperature below the martensite finish, M_f, temperature. This results in the Nitinol entirely in the martensitic phase state. When no stress is applied the martensite is in what is called the twinned configuration, and the strain is approximately 0. When a stress is applied the Nitinol deforms through twinning and follows the curve to point B, where the Nitinol part is strained to approximately 8% strain. Nitinol in the martensite phase is very soft and can be easily deformed by detwinning [8]. Twinning is a dislocation mechanism that rearranges the crystal structure to different twin variants as strain goes up [5]. Martensite Nitinol has 24 possible twin orientations, making deformation by twinning

easier than conventional metals such as stainless steel via dislocation movement of the crystal structure [5]. The Nitinol at point B is still in the martensitic phase, however now detwinned with the “kinks” seen in the twinned orientation are no longer present. When the stress is removed, most of the deformation on the part is maintained and Nitinol is still detwinned, illustrated by the path from point B to point C. When the Nitinol is subject to heat, the Nitinol shape starts to change from a martensitic phase to an austenitic phase and returns to the shape prior to the stress being applied. The return to the original shape starts at the austenite start, A_s, temperature and returns to the original shape once subject to a temperature greater than or equal to the A_f temperature. Cooling the part back down to a temperature below the martensite finish temperature would return the Nitinol to the martensite twinned state, point A and the cyclical process can start again. The cycle connecting points A, B, C, D and back to A illustrates the concept of shape memory.

The phase transformation between austenite and martensite not only occur when the material is subject to external stimuli such as a change in temperature (shape memory), but also when a stress is applied/deformation occurs (superelasticity). Above the A_f temperature, but below the martensite deformation temperature, M_d, Nitinol has superelastic behavior. The superelastic nature of Nitinol causes martensitic regions to form where stress is applied, despite the environment having a temperature higher than where the martensite phase typically occurs. In Figure 1, the superelastic cycle starts at point O. When a stress is applied, the stress strain curve follows the non-linear loading curve to point E. The observed loading curve is due to the stress-induced phase transformation of the Nitinol from the austenite phase to the martensite phase. The phase transformation to

martensite starts at the inflection point where the first linear elastic region ends, and the plateau region begins. The phase transformation to martensite finishes once the second inflection point is reached around 8% strain, between the end of the plateau region and beginning of next linear elastic region. As soon as the stress is removed the martensite immediately reverts to the undeformed austenite state which provides the springy, “rubber like” elastic behavior [9]. The unloading curve plateaus at a lower stress and shape recovery occurs via the reduction in stress without the application of heat [9]. In addition to this phenomenon, the superelastic definition can be derived from the high recoverable strain, when compared to stainless steels have much lower recoverable strains where the elastic limit is less than 1%. Where most metals can tolerate only a small fraction of a percent of strain without permanent deformation (<1% for most stainless steels), Nitinol routinely can withstand high strain (6-8% strain) and afterward return to its original shape without noticeable residual strain [10]. This behavior makes Nitinol feel very “springy” and able to return to its original form even after strains up to 8% are applied, making it known for its high fatigue life and fatigue strength.

Above the M_d temperature Nitinol no longer goes through a stress-induced phase transformation. The Nitinol can then no longer reach as high of a strain before plastic deformation or fracture. The stress at fracture is the UTS and the strain at fracture is the percent elongation. For testing conducted at a temperature above the M_d temperature, a 10% elongation at break is common.

2.1.2 Nitinol Phase Transformations

To control the unique properties of shape memory and superelasticity, knowing the heating transition temperatures of Nitinol is important. As previously shown in Figure 1, there are four phase transition temperatures associated to the reversible austenite-martensite transformations of Nitinol. However, the A_f temperature is the most studied because it is the temperature boundary separating the shape memory and superelastic behavior seen in Nitinol.

2.2 A_f temperature

The A_f transition temperature varies due to chemical composition of Nitinol and differences in how the Nitinol is processed. Chemical composition typically plays a larger role in A_f temperature but is typically controlled by the major Nitinol suppliers. A general trend can be seen in Figure 3 showing how the atomic mass percentage of nickel can cause a large difference in A_f temperature over a range of only 2% by weight.

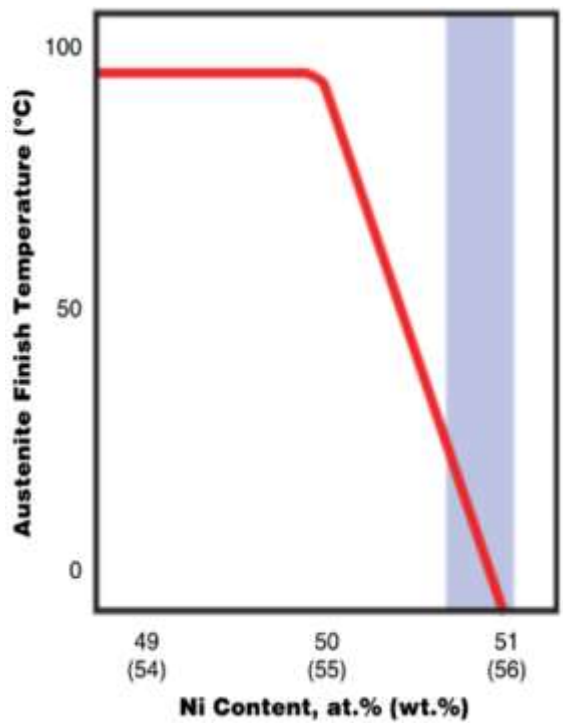

Figure 3: Graph showing effect nickel content has on the A_f temperature with the shaded region representing the nickel content most commonly seen in Nitinol provided from large suppliers. [11]

2.2.1 Adjusting A_f temperature

Once Nitinol is received there is still opportunities to tune the A_f temperature to a certain range through different heat treatment processing. When heat treating, Nitinol is cooled below M_f temperature and then deformed into a desired shape using a mandrel. The Nitinol mandrel is processed via the determined heat treatment parameters. This follows a general Nitinol heat treatment phase transformation cycle shown in Figure 4 starting with the austenite phase at the top of the triangle. This cycle is consistent with the previously described phase transformations from Figure 2.

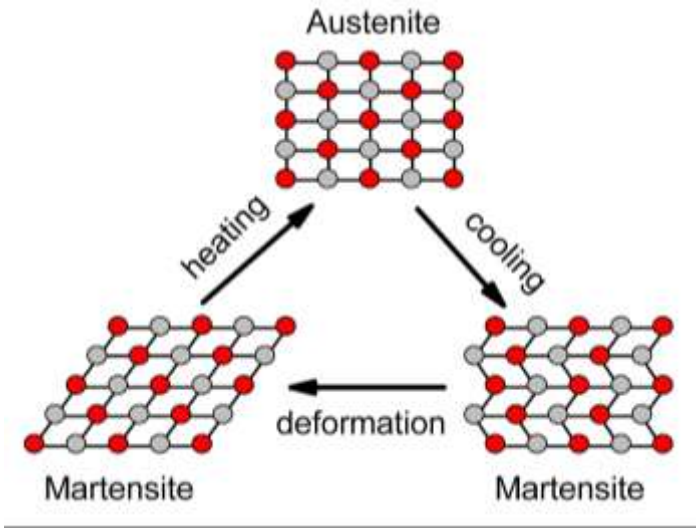

Figure 4: Simplified 2D view of Nitinol's crystalline structure during cooling/heating cycle [12]

When heat treating Nitinol, the wire transition temperatures change. Shifts in the process parameters will result in shifts in the transition temperatures similar to those seen in previous studies. Time-at-temperature also affects the wire properties. The more time-at-temperature the softer the wire and moves the mechanical properties of the wire closer to the fully annealed, while the shorter time-at temperature results in tensile behavior closer to the high-strength cold worked state [13]. Research investigating the heat treatment process and the resulting transformation temperatures change, namely the A_f temperature, of Nitinol wire after heat treatments of varying time and temperature have been conducted. Results from a few studies have shown that for heat treatment temperatures above 500°C, the A_f temperature tends to initially decrease with time before increasing and plateauing [13], [14].

2.2.2 Quantifying A_f temperature

Chemical analysis via nickel concentration by percent weight is not a precise enough method to directly correlate or measure the transformation temperatures. Therefore, testing through thermal analysis is done to accurately determine transformation temperatures of samples with a known thermal history. Differential Scanning Calorimetry (abbreviated DSC) and Bend Free Recovery (abbreviated BFR) testing are the two most common thermal analysis methods in determining transition temperatures (namely A_f transition temperature) post processing. The A_f temperatures can be determined post-processing using the DSC in accordance with ASTM 2004-17 [13], [15]. DSC provides a rapid method of determining the transformation temperatures of nickel titanium shape memory alloys using a small stress-free, annealed sample of Nitinol. Preparation of the DSC sample is also very important. Samples are 25 to 45mg and should be cut to maximize surface contact to the DSC sample pan. However, cutting and grinding can cause localized heating and/or deformation that affect the transformation temperature [15]. The A_f temperatures can also be determined post-processing using the BFR Method [14] in accordance with ASTM F2082-16 [16]. This method involves cooling a test specimen to the fully martensitic phase, deforming the specimen and heating the specimen to the above the A_f temperature. During heating, the specimen deformation is measured and plotted versus temperature. The tracking of the specimen deformation is usually measured using a vision system or variable differential transformer. The variable differential transformers come in two types: LVDT and RVDT. LVDTs measures linear displacement while RVDT

measures angular displacement. Both DSC and BFR test methods measure the same output; however, results are oftentimes offset by a few degrees due to the nature of the sample preparation. It should be noted that the DSC and BFR measurement difference is oftentimes due to the effects of strain and load on the transformation. In addition, the heat usually added to the sample when cutting to the appropriate size for DSC results in a slightly higher A_f temperatures than the A_f temperature obtained through the BFR test method.

2.3 Nitinol Processing Equipment

Fluidized sand bath, fluidized salt baths and furnaces/ovens are the three most commonly chosen equipment for Nitinol heat treatment processes. Fast transitions from cold temperatures (room temperature) to the selected heat treatment temperature and a fast transition from the heat treatment temperature back down to the cold temperature is oftentimes desired for more process and output control (namely the A_f temperature). This is commonly analyzed either with a thermocouple logging temperature data during a heat treatment or evaluation of the A_f temperatures.

2.3.1 Sand Bath

The sand bath use conduction to transfer heat to the Nitinol using fine sand. Heating elements run along the sides of the bath. The cooling media used for fast cooling of the Nitinol after the heat treatment is typically cold sand or deionized water. A gas is used to mix the hot sand. Colder pockets of the gas used have the potential to contact the part. This causes the part to see fluctuating temperatures during the heat treatment process. This is

evident in the sand bath traces oscillating after the initial rise to the heat treatment temperature and before the drop down to the cooling temperature to stop the material from continued exposure to the hotter temperature range that causes the material property changes. See Appendix A to see the sand bath heat treatment traces.

2.3.2 Salt Bath

The typical salt bath also uses conduction to transfer heat to the Nitinol using molten salt. The cooling media used for fast cooling of the Nitinol after the heat treatment is typically deionized water. The means to keep the molten salt temperature homogeneous throughout the salt bath is a stirrer. This avoids the potentially negative impact cold pockets of gas have on parts when heat treated in the sand bath. The salt bath is also too viscous for air to flow from the bottom of the bath to the top. The salt bath also heats the parts faster and maintains a more consistent temperature. This is evident in the salt bath heat treatment traces seen in Appendix A.

2.3.3 Furnace/Oven

Furnaces and ovens use convection to transfer heat to the Nitinol. Hot air is circulated around the parts however all parts. The cooling media used for fast cooling of the Nitinol after the heat treatment has been completed is typically deionized water or cooling fans. The key downfall of this method is the loss of heat from the opening of the oven door when placing a Nitinol part in the oven. The oven is therefore more practical when heat treating for long periods of time (greater than 1 hour) and lower heat treatment temperatures (below 400°C); when the time it takes for the equipment to settle back to the

heat setting is not as critical. This is seen in previous studies showing trends of Nitinol behavior after heat treatments for 60 or 180 minutes [13].

2.4 Nitinol Wire Tensile Testing

Pull tests procedure are typically performed in accordance with ASTM F2516-14 [17]. Using the conventional tensile testing, samples were pulled to 6% strain and the unloaded to less than 7MPa, and then pulled to failure. The mechanical properties are defined in the standard and definitions for the mechanical property parameters of interest for the tensile testing are provided in Figure 5.

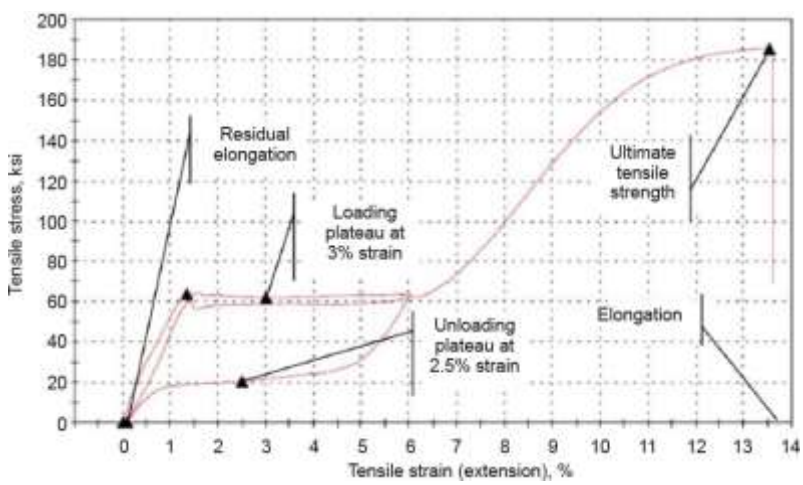

Figure 5: Definitions for Mechanical Property Parameters of Interest [18]

Stresses are measured at certain strains along the curve and strains are measured at the end of loading (residual elongation) and strain at failure (elongation). Testing was done at body temperature of 37°C, this is different from the default temperature called out in the standard of 22 +/- 2°C. Previous studies have shown tensile property trends after parts were

heat treated to different time and temperatures of Nitinol wire in a furnace and salt bath over a large range of times and temperatures [13], [14]. It is very common however for companies in the medical device industry to heat treat parts for short periods of time, less than 5 minutes. Focusing more attention to shorter time periods and a smaller range of temperature values is more useful when building off published data and understanding trends on a more micro scale pertinent to realistic times used in industry than trends seen at a macro scale that has been highlighted in previous studies.

The radial resistance force is the radial force to compress the stent to a smaller diameter, usually loading the stent into a catheter. The chronic outward force is the force the stent exerts on the surface when expanding back to the original diameter, usually when delivering a stent from its catheter into the native annulus location. As shown in Figure 6, radial resistance force is derived from the upper plateau strength and the chronic outward force is derived from the lower plateau strength. In most applications, it is best to have the largest difference between the upper and lower plateau strengths for better fatigue life (UPS and LPS, respectively).

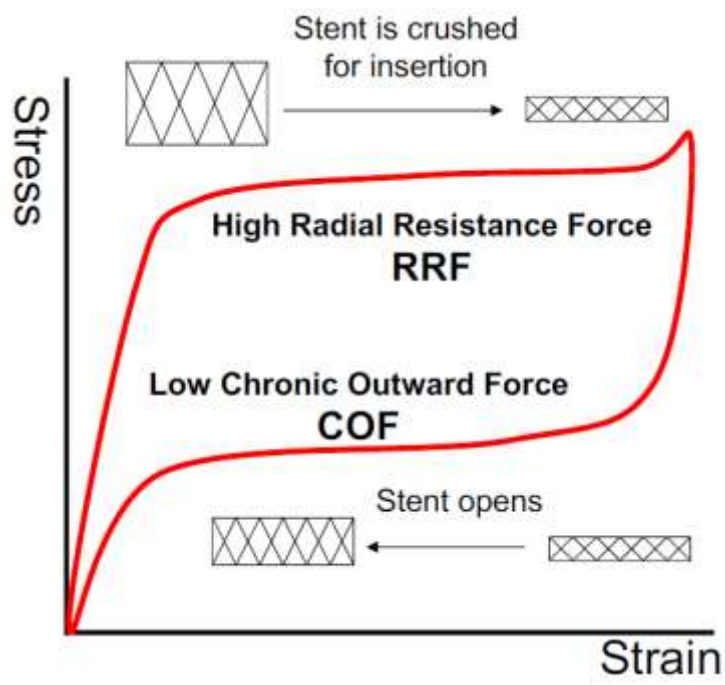

Figure 6: Graphical representation of the typically desired radial resistance force and chronic outward force when considering the Nitinol hysteresis when temperature is above the A_f temperature. [21]

2.5 Summary

In summary, studies have been conducted comparing the effect of different Nitinol wire heat treatment methods/parameters or the effect of different Nitinol wire processing on tensile data. The effect of the heat treatment equipment/media has not been investigated in much detail. The purpose of this study is to fill this gap by analyzing the mechanical behavior differences between Nitinol wire heat treated in a salt bath and Nitinol wire heat treated in a sand bath. Equipment is expensive and knowing if one is superior is helpful for companies looking to produce viable medical devices that use Nitinol. The improved performance when comparing equipment has the potential to result in better patient outlook

and treatment in the medical field for many devices including critical Class III devices like prosthetic heart valves. Risk mitigation and improved quality using equipment that is more repeatable and reproducible is also an important consideration. This study will investigate the different heat treatments that could be used to improve the mechanical properties of the HLT Meridian transcatheter aortic valve through Nitinol heat treatment processing. The most relevant mechanical properties (UPS, LPS, UTS, Residual Elongation and Elongation) and the A_f temperature will be the outputs of most interest when evaluating the differences in the heat treatment equipment, time and temperature settings. The lessons learned and methods used will also be able to be applied to other Nitinol medical devices and other Nitinol-based inventions.

3 Experimental Procedure

This chapter presents details on the Nitinol material used in this study, the experimental methods used to characterize the wire thermal and mechanical properties, and data analysis methods by which the data will be interpreted.

3.1 Nitinol Wire Sample Preparation

Wire from one spool of Fort Wayne 0.011" Nitinol wire was used in this study to prevent the effect of uncontrolled variables present in lot variations such as, wire transformation temperatures before processing, chemical composition (percentage nickel and titanium) and cold work percentage. The Nitinol wire came wrapped around an eight-inch diameter spool. Nitinol wire was taken from the spool and cut to length. Each wire was placed on the stainless steel 17-4 PH mandrel as shown in Figure 7. Each end of the wire is clamped down with no tensile load applied to samples prior to the heat treatment. The Nitinol wire was not shielded from the heat treatment media zero mass around sample tested. The mandrel holds four wires at a time. Three samples for tensile testing and one sample for transition temperature testing.

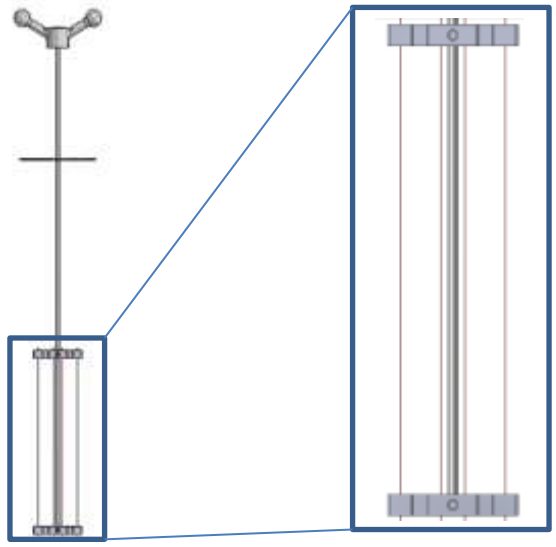

Figure 7: Tensile Sample Mandrel

All four wires are assumed to experience the same heat treatment when processed at the same time. Samples were placed in the heat treatment equipment (sand bath and the salt bath) at a similar height for all sample groups as shown in Figure 8.

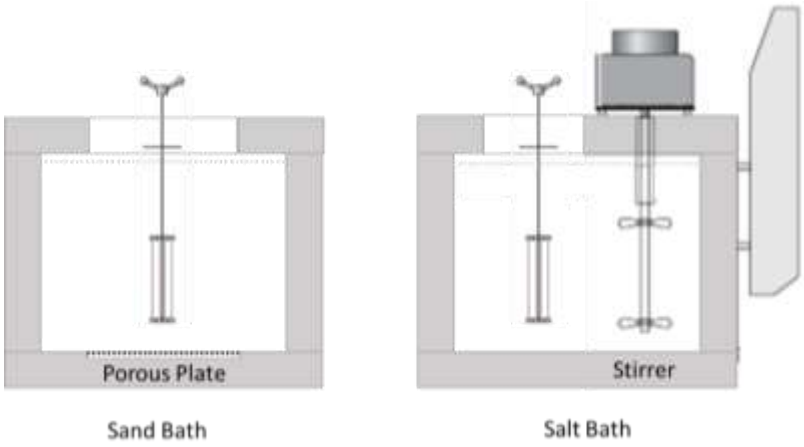

Figure 8: Sample Mandrel Placement in Sand Bath VS Salt Bath

Salt bath samples were heat treated at specified temperatures for specified times in a Fluke 6050H High Temperature Salt Bath. Sand bath samples were heat treated for the

same specified temperatures and specified times in a Techne FB-08C Sand Bath. The salt bath media used was a trade secret pink solid salt comprised of potassium nitrate, sodium nitrite and sodium nitrate among other trace chemicals from Fluke Calibration. A stirrer is built into the salt bath, to mix and ensure temperature is homogenous throughout the salt bath media. The sand bath media was comprised of 100% Aluminum Oxide from Accurate Thermal Systems. The sand uses a different method to agitate the heat treatment media; air with 60 psi of pressure passes through a porous plate at the bottom of the sand bath and bubbles to the top of the media. A calibrated Omega thermocouple was used to monitor the heat treatment temperature throughout each specimen's heat treatment. A baseline temperature reading was read for 30 seconds prior to placing the mandrel in the equipment and continued through the end of the heat treatment process. After placing the samples in the heat treatment equipment all samples were quenched in deionized water 6 seconds after removal of the mandrel from the equipment. This provided ample time for a gentle shake of the mandrel returning most of the media (sand/salt) carried out of the equipment by the mandrel to drip back in before quenching. The mandrel remained in the deionized water tank for two minutes.

Traces were performed to determine if there were large differences in the temperature of the sand bath vs salt bath media during processing.

3.2 Mechanical Testing

3.2.1 Tensile Properties

Following the heat treatment process, the regions of wire that were constrained to hold the wire in place during the heat treatment process were cut off the final sample by cutting the part free between the mandrel grips (Figure 9). Sample length post cut was a minimum length of 6” per testing standard set by Fort Wayne’s testing protocol and ASTM F2516. The diameter of each sample was measured and recorded to the nearest 0.0001” using a laser micrometer. Tensile testing was performed on an Instron tensile tester (TT-10) equipped with a 225-lbf axial load cell (LD-225G). The tests were performed in a temperature controlled environmental chamber controlling test temperature to within 1°C of typical body temperature (37°C). Displacement was monitored by video extensometer. Pneumatic cord grips were used to hold each end of the wire through the duration of the test. Specimens were tested with a 3-inch gage length between pneumatic cord grips and 2-inch gage length between video markers. Strain was determined from displacement measurements and effective length of the sample prior to initiation of the test. Strain rate was set to 0.5 in/min for the entirety of the test.

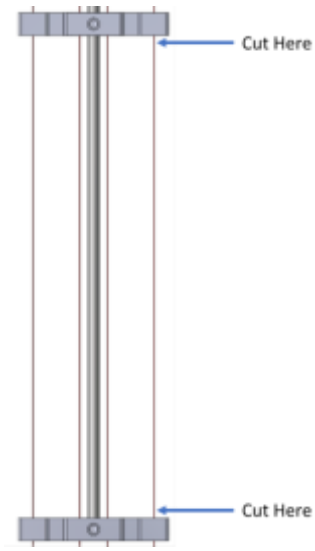

Figure 9: Specimen Cut Locations

As specified in ASTM-F2516, the specimen was extended to 6% strain, prior to unloading to 0 psi stress in the first cycle of the test. See Figure 6. The upper and lower plateau strengths were determined at 3% strain during loading and 2.5% strain during unloading, respectively. The test specimens were then loaded to break during the second loading cycle. Stress exhibited on the wire was calculated using the load data and diameter of wire specimen determined before testing.

3.3 Thermal Analysis

3.3.1 DSC Testing

DSC testing was conducted to determine the Af transition temperatures of Nitinol. A small sample was cut from the device (less than <50mg). The difference in the amount of heat required to increase the temperature of the control and the sample was measured as a function of time.

An ideal result showing the four transition temperatures and peak heat flow for the austenite and martensite of Nitinol is shown in Figure 10.

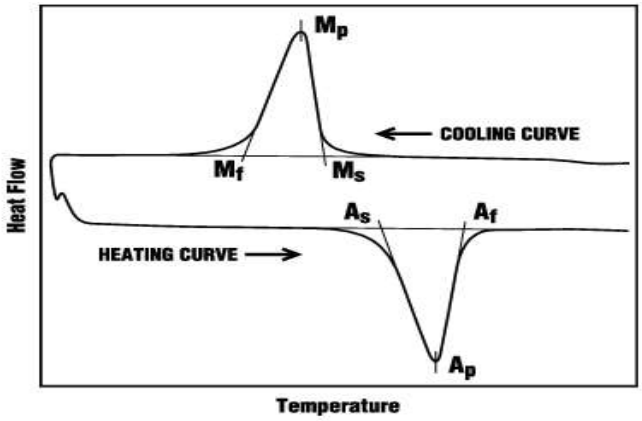

Figure 10: Heat Flow Curve of Nitinol seen in DSC Testing [19]

3.4 Statistical Analysis

3.4.1 Minitab Analysis

Statistical analysis was performed using the Regression Model function in Minitab to determine whether the means of different sample groups differ. The Regression Model is an analysis of variances (ANOVA) procedure in which the calculations are performed using a least squares regression approach to describe the statistical relationship between the different process parameter inputs and the mechanical properties. Regression analysis generates an equation/model to describe the statistical relationship between one or more predictor variables (time, temperature and heat treatment equipment) and the response variable (the tensile mechanical properties). Residual plot analysis is performed in order to validate the equation/model. This is done to account for the effect of randomness and unpredictability, crucial components to the validity of any regression model. One

assumption made when conducting regression model tests is that the sample population must be close to a normal distribution. Regression analysis, normal probability plots and checking the goodness of fit R-squared values were used to ensure the sample populations were close to normal. Normal probability plots were evaluated visually, looking for curves in the data that would represent a skew, S-curves representing short or long tails in the normal distribution or outliers in the data. P-values less than 0.05 for the analysis of variance signified variables that had a statistically significant impact on the value of the mechanical property analyzed. Further evaluation investigated removing input variables that were not significant in attempt to eliminate noise caused by the insignificant variable(s) and provide a better model. A goodness of fit R-squared values standard was set to have all three R-squared values within 10% of each other and the R-squared predicted value above the 60% value indicated the model could be used to predict the value of mechanical properties. The data was first grouped by independent variables heat treatment time, heat treatment temperature and heat treatment equipment. The same data was grouped a second time by A_f temperature, heat treatment temperature and heat treatment equipment.

4 Results

In this chapter, results and analysis for the mechanical and thermal tests are presented. First, the tensile parameter results are presented for the Nitinol wire heat treated in the different equipment and for different time and temperature settings. Next the thermal test results are provided for analysis as a known factor in the tensile property behavior are provided.

The salt bath typically heats the Nitinol sample faster and holds temperature better than the sand bath, especially when mandrel mass is high, and the Nitinol part is shielded from direct contact to the heat treatment media. However, in a very low mass/no shielding scenario the difference between the heat treatment in the sand bath versus the salt bath may not be as large. Traces using a calibrated type K thermocouple showed that the salt bath parts were exposed to slightly higher temperatures (~3°C). The salt bath traces also looked more consistent during the heat treatment; the sand bath traces showed temperature fluctuations. It is believed that the temperature fluctuations read by the thermocouple were caused by cold pockets of air that flowed from the porous plate out of the top of the sand. The salt bath traces did not show fluctuations, as a stirrer is used instead of air to keep the media temperature homogeneous throughout the bath. Traces at 485°C for 1 minute was done with no mandrel/only thermocouple was done to further prove this theory and identify any further differences between the heat treatment equipment not associated with the experiment/testing. The traces also peaked close to the set equipment temperature before dropping down a few degrees, which is hypothesized to be a mechanism in how the thermocouple reads temperature. Two traces were done in each heat treatment equipment.

The thermocouple was placed at two different depths: the first trace had the thermocouple in the media approximately the same depth as it was for the heat treatment of the tensile samples and the second trace had the thermocouple less than 1 inch deep from the surface of the media. All temperature traces are provided in Appendix A. The depth of the thermocouple resulted in approximately a 1°C to 2°C difference in the temperature read by the thermocouple. This temperature difference can be attributed to the measurement error when using a thermocouple. Error arises from the loss of heat up the stem of a thermocouple through conduction or convection which can prevent the measuring junction of the thermocouple from reaching the temperature of its surroundings [20].

The small variability in the diameter was determined to not have on any of the mechanical properties investigated. In general, diameter is known to have an impact on all the mechanical properties, however for a small enough sample diameter range from 0.01114" to 0.01122" no statistically significant impact was observed. This was to be expected based on the tensile strength stress equation for an ideal wire in which the stress and diameter are inversely related:

$$\sigma = \frac{F}{A} = \frac{F}{\pi * \left(\frac{d}{2}\right)^2} \tag{1}$$

The stress of a wire with a diameter of .01114" is approximately 99% of the stress in the stress of a wire with a diameter of .01122", assuming all other properties are the same.

Tensile testing was performed to compare the stress-strain behavior of the different sample groups. The analysis of the results provide insight into the effect of time,

temperature and heat treatment equipment on the mechanical behavior. Tensile results were taken for eighteen sample groups with three replicates for each group. The mechanical properties: upper plateau strength, lower plateau strength, residual elongation, ultimate tensile strength, and elongation at break were all tested and recorded per ASTM 2516. The raw data for the sand bath and salt bath samples can be found in Appendix B and Appendix C, respectively. Normal probability plots of the residuals and R-squared goodness of fit values were evaluated for the five different mechanical properties to ensure data could be modeled to predict future tensile results. The results were analyzed to ensure that the statistical analysis plan was still appropriate. The mechanical properties were then compared to a previous process to obtain a more optimal process that gives desired improvements to the tensile properties of the Nitinol wire.

4.1 Optimal Tensile Properties

High delivery forces related to the radial resistance force in the HLT Meridian transcatheter aortic valve, a lower UPS is desired for the new process (mean UPS less than 89,888 psi). A lower chronic outward force for higher fatigue resistance and to reduction of conduction issues that cause arrythmias in the heart from high radial force exerted by the implanted valve against the native aortic valve and surrounding heart tissue results in the need for a lower LPS (mean LPS less than 43,220 psi). The new process should also have a residual elongation less than 0.10% to improve the permanent deformation from loading and unloading of the valve in the delivery catheter. Higher Ultimate Tensile Strength (212,372 psi) and Elongation (18.0%) are also desired for greater design space of stronger and more ductile wire. High process repeatability and reliability is also an

important consideration when selecting a process and equipment. The HLT process and corresponding tensile data obtained following 3.2.1 are summarized in the Table 1.

Table 1: Process used for the HLT Meridian transcatheter heart valve

Description	Diameter (in)	Upper Plateau Strength (psi)	Lower Plateau Strength (psi)	Residual Elongation (%)	Ultimate Tensile Strength (psi)	Elongation (%)
Sand Bath 525°C 2 min	0.01114	88,095	42,591	0.12	209,093	18.0
	0.01114	92,247	44,689	0.11	218,141	18.0
	0.01114	89,324	42,381	0.08	209,883	17.9

4.2 Stress Parameters Tensile Testing

4.2.1 Upper Plateau Strength

Figure 11 and Figure 12 show the upper plateau strength of the different sample groups for the sand bath and salt bath, respectively. The general upper plateau strength trend shows as time and/or temperature increase the upper plateau strength decreases. Time had a larger statistical impact on the upper plateau strength than temperature. There is no evidence that would refute the hypothesis that the heat treatment equipment did not have a statistically significant impact on upper plateau strength. The variability of the sand bath parts and salt bath parts were similar for parts heat treated at 485°C and 525°C, however salt bath parts heat treated at 505°C had very little upper plateau strength variability within time and temperature groups (less than 2,000 psi) for the entire time range as opposed to sand bath parts that spanned a larger range.

Only a few sample groups met the specification of an upper plateau strength less than 89,888 psi. The samples heat treated at 525°C for 2 minutes and 3 minutes passed the specification for both the sand and salt bath. Samples heat treated at 505°C for 3 minutes

in the salt bath passed the specification. In addition, when only considering the mean of the sample group, parts heat treated in the sand bath for 505°C for 3 minutes passed the specification. The mean for the sand bath for 505°C for 3 minutes sample group is 88,337 psi.

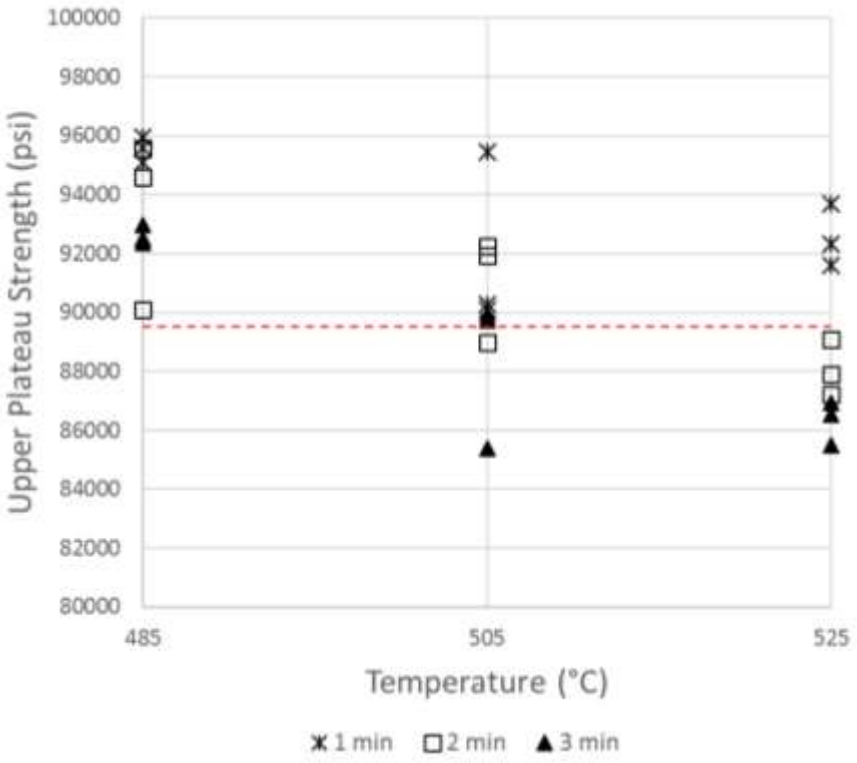

Figure 11: Upper Plateau Strength (UPS) Individual Value Plot grouped into heat treatment parameters for samples heat treated in the sand bath. Dashed line refers to the average UPS for the current HLT process.

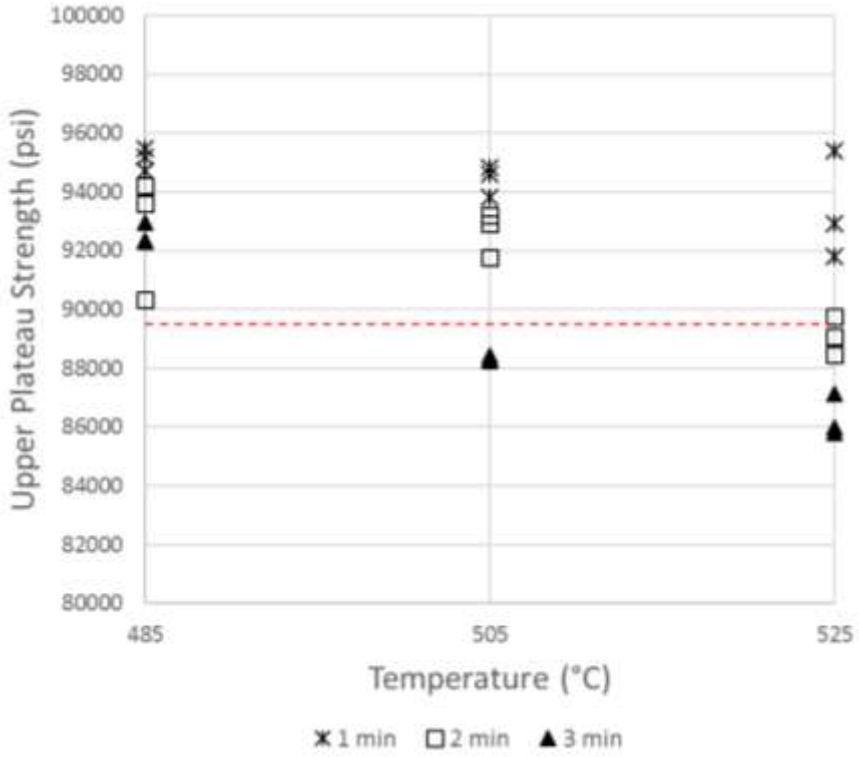

Figure 12: Upper Plateau Strength (UPS) Individual Value Plot grouped into heat treatment parameters for samples heat treated in the salt bath. Dashed line refers to the average UPS for the current HLT process.

A regression ANOVA analysis of the different mechanical properties was performed in Minitab. When evaluating the upper plateau strength, the heat treatment equipment showed the heat treatment equipment variable was not found to be statistically significant with a p-value of 0.234. Time and temperature variables all showed statistical significance with p-values less than 0.05. Time and temperature both possessed a p-value of 0.000. The goodness of fit R-squared values ranged from 70.37% to 74.48%. These values meet the standard set to give confidence in the upper plateau strength model for the

data range observed. The upper plateau strength normal probability plot of the residuals for 54 samples form a nearly linear pattern, showing no obvious skew (Figure 13). There are four points that form a curve at the left (lower) end of the probability plot that indicates that the normal distribution of the residuals has a long lower tail.

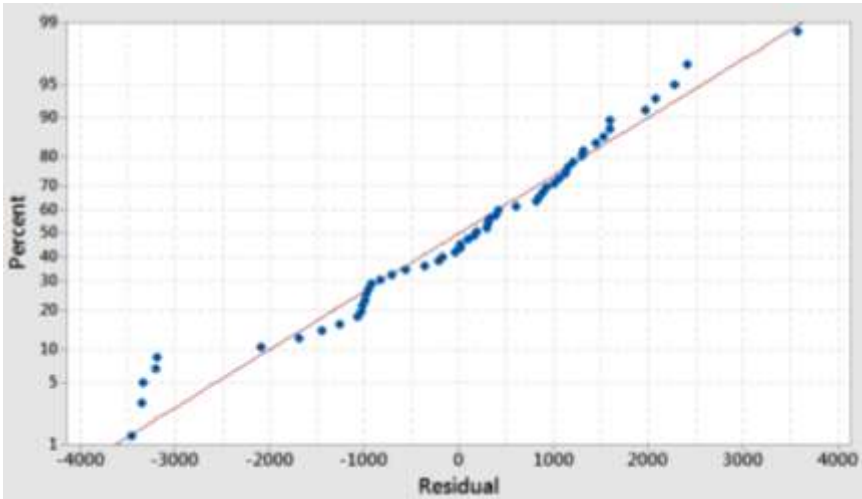

Figure 13: Upper Plateau Strength (psi) Normal Probability Plot of Residuals

4.2.2 Lower Plateau Strength

Figure 14 and Figure 15 show the lower plateau strength of the different sample groups for the sand bath and salt bath, respectively. The general lower plateau strength trend shows as time and temperature increase the lower plateau strength decreases. Time has a larger statistical impact on the lower plateau strength than temperature. There is no evidence that would refute the hypothesis that the heat treatment equipment has a statistically significant impact on lower plateau strength. The salt bath parts had less variability than the sand bath parts, with one part in most groups larger than the rest.

Only a few sample groups met the specification of a lower plateau strength less than 43,220 psi. The samples heat treated at 525°C for 2 minutes and 3 minutes passed the

specification for both the sand and salt bath. Samples heat treated at 505°C for 3 minutes in the salt bath passed the specification.

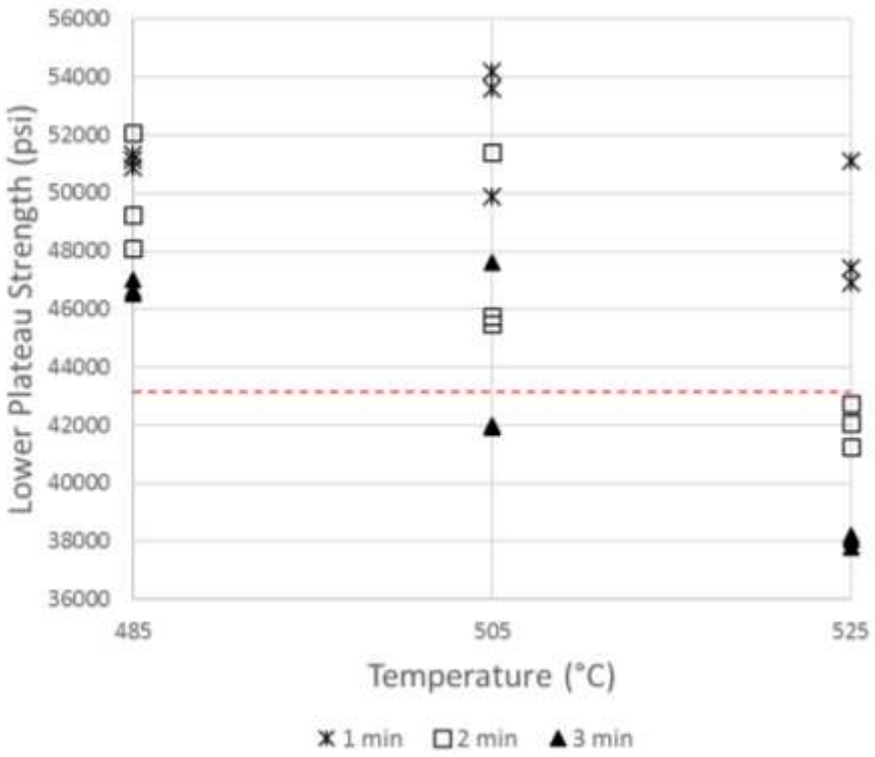

Figure 14: Lower Plateau Strength (LPS) Individual Value Plot grouped into heat treatment parameters for samples heat treated in the sand bath. Dashed line refers to the average LPS for the current HLT process.

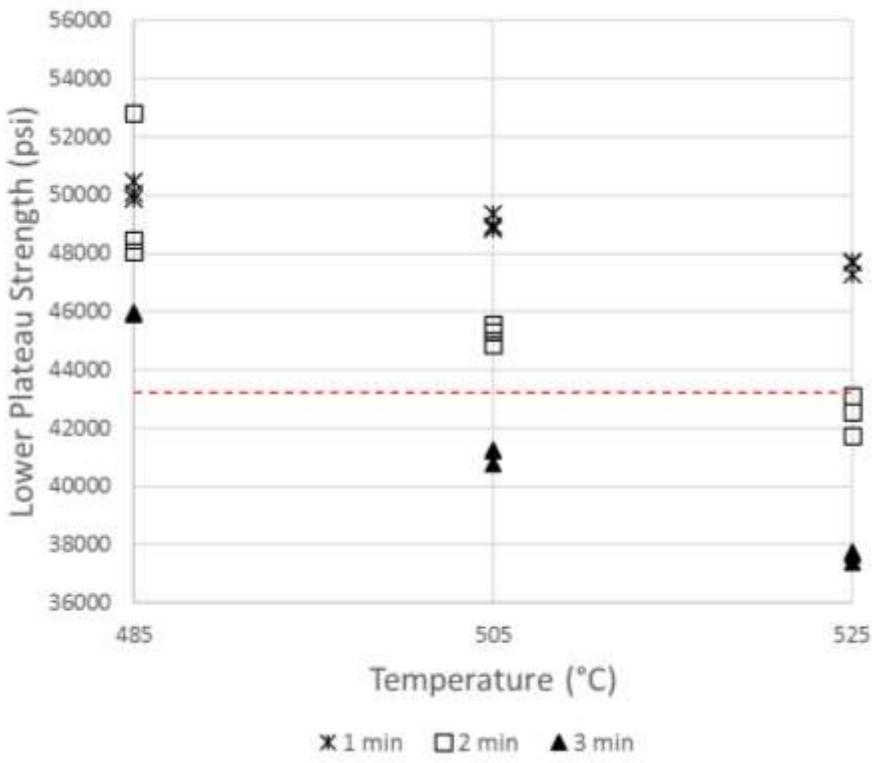

Figure 15: Lower Plateau Strength (LPS) Individual Value Plot grouped into heat treatment parameters for samples heat treated in the salt bath. Dashed line refers to the average LPS for the current HLT process.

A regression ANOVA analysis of the different mechanical properties was performed in Minitab. When evaluating the lower plateau strength, the heat treatment equipment showed the heat treatment equipment variable was found to be statistically significant with a p-value of 0.020. Time, temperature and heat treatment equipment all showed statistical significance with p-values less than 0.05. Time and temperature both possessed a p-value of 0.000. The goodness of fit R-squared values ranged from 80.33% to 83.08%. These values meet the standard set to give confidence in the lower plateau strength model for the data range observed. The lower plateau strength normal probability

plot of the residuals for 54 samples form a graph with plotted points bent down and to the right of the normal line which indicates a long tail to the left, skew left distribution (Figure 16).

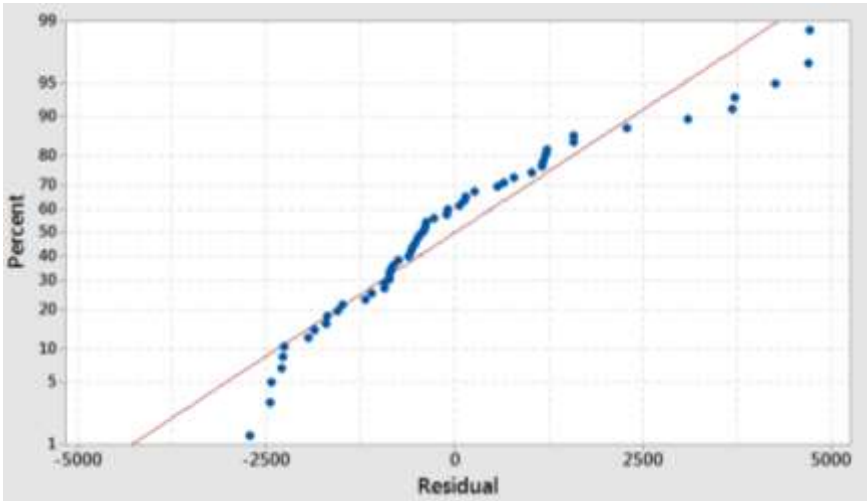

Figure 16: Lower Plateau Strength (psi) Normal Probability Plot of Residuals

4.2.3 Ultimate Tensile Strength

Figure 17 and Figure 18 show the ultimate tensile plateau strength of the different sample groups for the sand bath and salt bath, respectively. The general ultimate tensile strength trend shows as time and temperature increase the ultimate tensile strength decreases. Temperature had the largest impact on the ultimate tensile strength. There is no evidence that would refute the hypothesis that the heat treatment equipment has a statistically significant impact on the ultimate tensile strength. For the same time and temperature sample group, the sand bath samples had slightly higher ultimate tensile strength than the salt bath samples (sample group means within 5000 psi of each other). All sample groups had low variability (less than 2500 psi) for all sample groups independent of time, temperature and heat treatment equipment.

Most of the sample groups met the specification of an ultimate tensile strength greater than 212,372 psi. All sample groups for the sand bath heat treated at 485°C and 505°C and the sample group heat treated for 1 minute at 525°C passed the specification. All sample groups for the salt bath heat treated at 485°C and 505°C passed the specification.

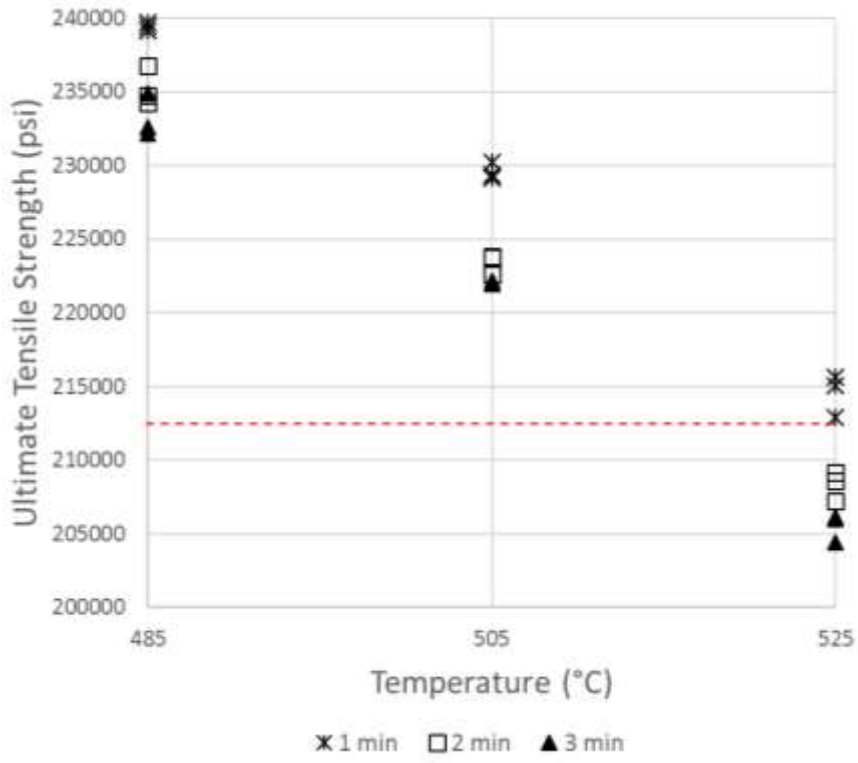

Figure 17: Ultimate Tensile Strength (UTS) Individual Value Plot grouped into heat treatment parameters for samples heat treated in the sand bath. Dashed line refers to the average UTS for the current HLT process.

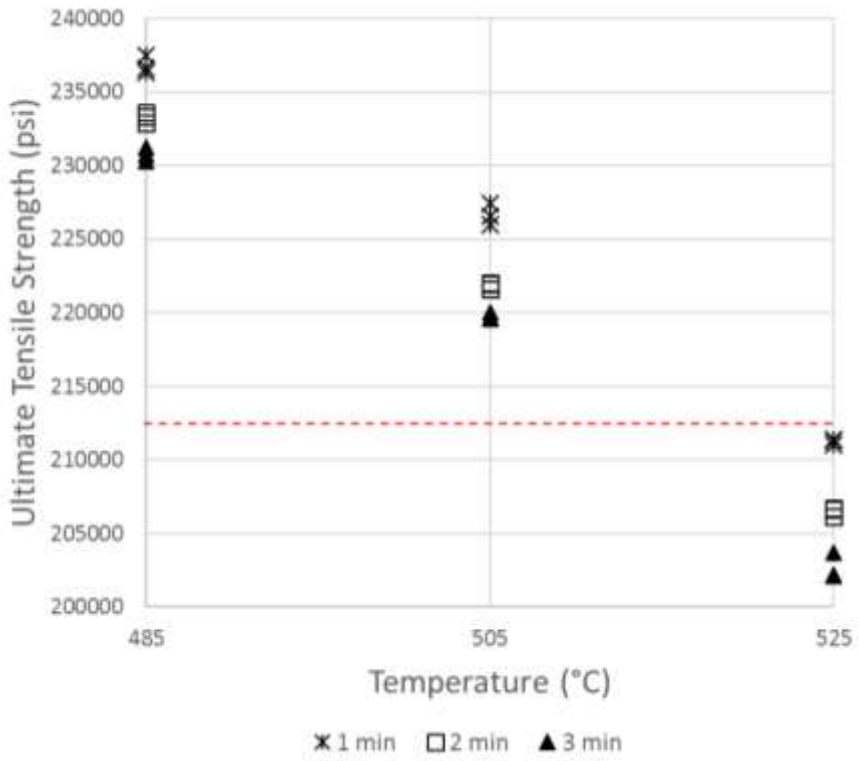

Figure 18: Ultimate Tensile Strength (UTS) Individual Value Plot grouped into heat treatment parameters for samples heat treated in the salt bath. Dashed line refers to the average UTS for the current HLT process.

The regression ANOVA analysis for the ultimate tensile strength showed the heat treatment equipment variable was found to be statistically significant with a p-value of 0.000. Time, temperature, and heat treatment equipment all showed statistical significance with p-values less than 0.05. Time, temperature and heat treatment equipment all had p-values of 0.000. The goodness of fit R-squared values ranged from 97.90% to 98.19%. These values meet the standard set for this testing which results in confidence in the ultimate tensile strength model for the data range observed. The ultimate tensile strength normal probability plot of the residuals for 54 samples form a curve which starts below the

normal line, bends to follow it, and ends above it indicates long tails. That is the variance is higher than expected in a normal distribution (Figure 19).

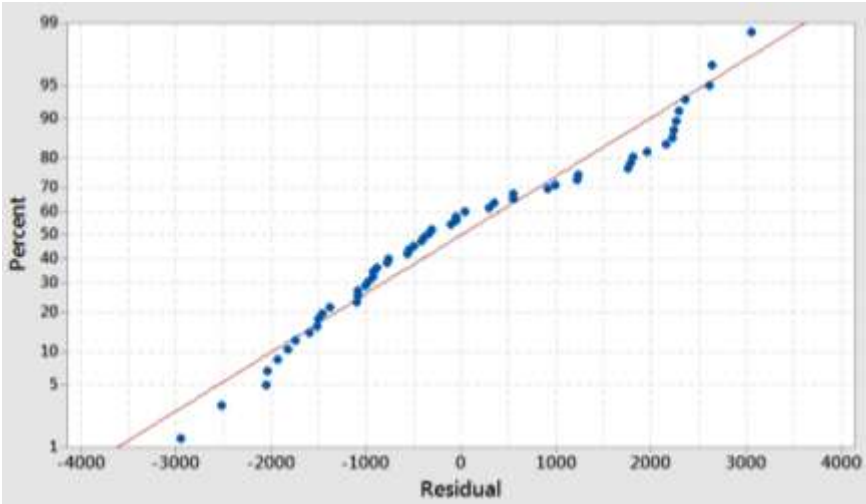

Figure 19: Ultimate Tensile Strength (psi) Normal Probability Plot of Residuals

4.2.4 Stress-Based Mechanical Properties Summary

To summarize, all stress-based mechanical properties were modeled with goodness of fit numbers above 60%, giving confidence in the conclusions made for general trends that that could be used to predict the stress values from known process inputs for the range of values tested. Both time and temperature had a statistical impact on all stress-based mechanical properties (lower plateau strength, upper plateau strength and ultimate tensile strength). Both time and temperature were inversely related to the different stress-based mechanical properties, following the general trend seen in literature that samples heat treated at higher temperatures and for a longer time results in lower strength values due to degradation of the wire [13], [14]. Time had the larger statistical impact on the upper plateau strength and lower plateau strength than temperature. Temperature had the largest impact on the ultimate tensile strength. The heat treatment equipment showed a statistically

significant impact in the lower plateau strength and ultimate tensile strength. Samples heat treated in the sand bath had higher stress values than the samples heat treated in the salt bath. The heat treatment equipment had the smallest impact on the three strength mechanical properties when compared to time and temperature. It is unclear why the heat treatment equipment did not have a significant impact on the upper plateau strength.

4.3 Strain Parameters Tensile Testing

4.3.1 Residual Elongation

Figure 20 and Figure 21 show the residual elongation of the different sample groups for the sand bath and salt bath, respectively. The sand bath and salt bath showed different trends for residual elongation. The parts heat treated in the salt bath do not appear to have any clear trends with regards to changes in time, temperature or heat treatment equipment. The large spread in the limited sample size makes it difficult to see clear trends. However, weak trends can be seen for samples heat treated in the sand bath: the residual elongation looks to be increasing with increasing temperature. The sand bath samples were not stable with high variability making it difficult to determine links differences in residual elongation to changes in the process parameters.

As stated above the sand bath samples have high variability which makes it difficult to draw conclusions to which sample groups will meet the desired residual elongation (below 0.10% residual elongation). All sample groups heat treated at 525°C in the sand bath had mean residual elongations greater 0.10%. Only one sample heat treated at 525°C in the sand bath had a passing residual elongation (0.08%). Most samples for the salt bath

samples were meeting the desired residual elongation and had little variability within sample groups. With only one sample in the sample group heat treated at a temperature of 505°C for 2 minutes having a residual elongation of 0.11%.

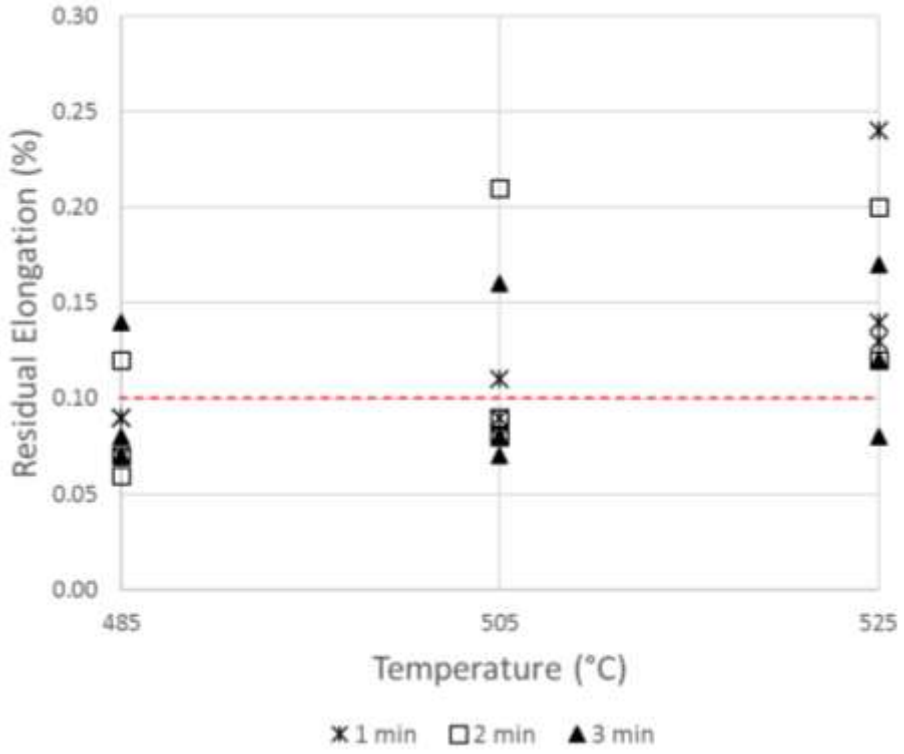

Figure 20: Residual Elongation Individual Value Plot grouped into heat treatment parameters for samples heat treated in the sand bath. Dashed line refers to the average Residual Elongation for the current HLT process.

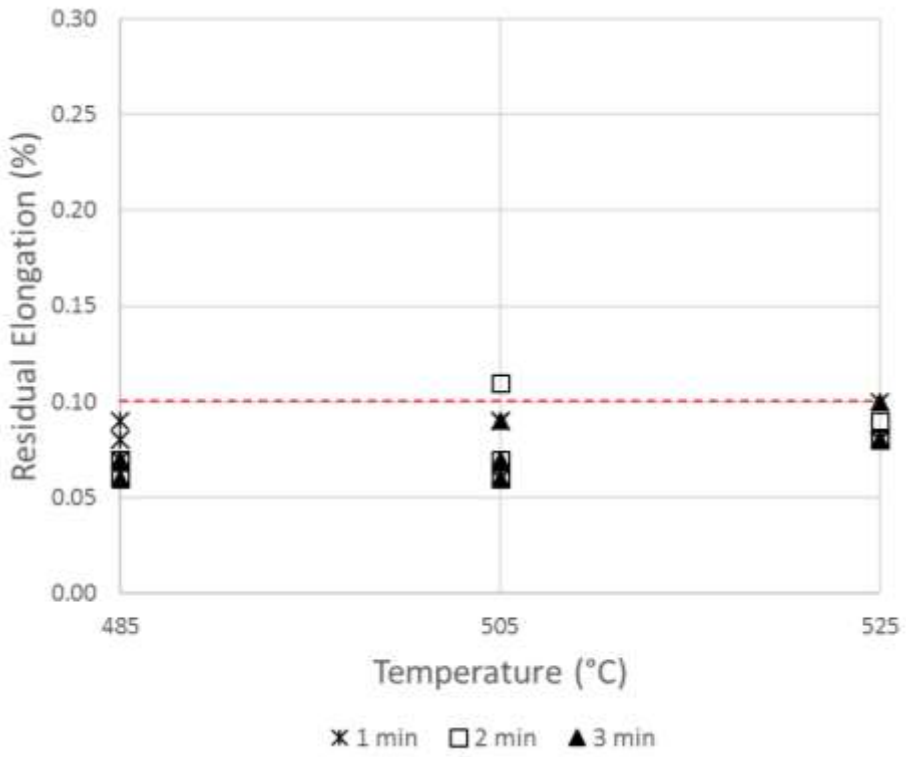

Figure 21: Residual Elongation Individual Value Plot grouped into heat treatment parameters for samples heat treated in the salt bath. Dashed line refers to the average Residual Elongation for the current HLT process.

The regression ANOVA analysis for the residual elongation showed the heat treatment equipment variable was found to be statistically significant with a p-value of 0.000. Temperature and heat treatment equipment all showed statistical significance with p-values less than 0.05. Temperature and heat treatment equipment had p-values of 0.000. Time had a p-value of 0.481 which represents time not having a statistically significant impact on residual elongation. The goodness of fit R-squared values ranged from 31.36% to 40.67%. These values do not meet the standard set for this testing which results in a decrease in confidence in the residual elongation model for the data range observed. The

residual elongation normal probability plot of the residuals for 54 samples shows the plotted points bending down to the right of the normal line which indicates a long tail to the left (left skew pattern) (Figure 22).

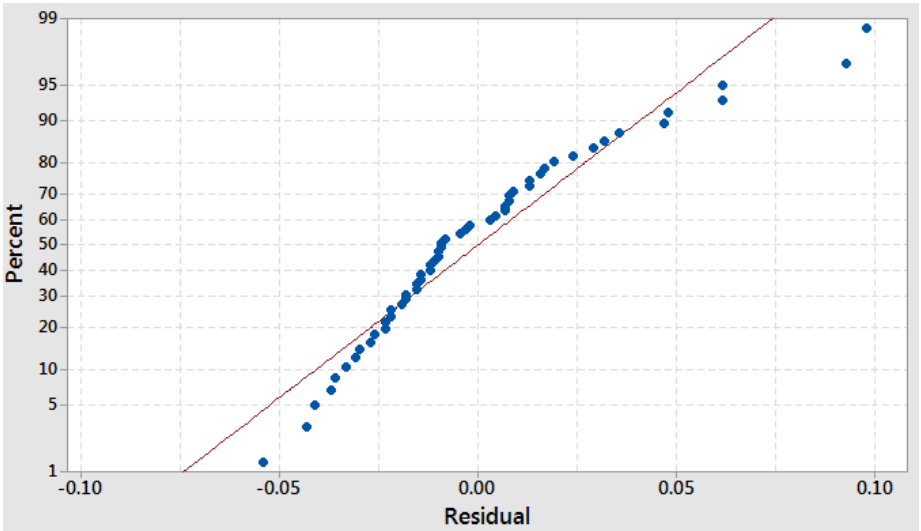

Figure 22: Residual Elongation (%) Normal Probability Plot of Residuals

4.3.2 Elongation

Figure 23 and Figure 24 show the elongation of the different sample groups for the sand bath and salt bath, respectively. The parts heat treated in the sand bath do not appear to have any clear trends with regards to changes in time, temperature or heat treatment equipment. The large spread in the limited sample size makes it difficult to see clear trends with regards to the inputs.

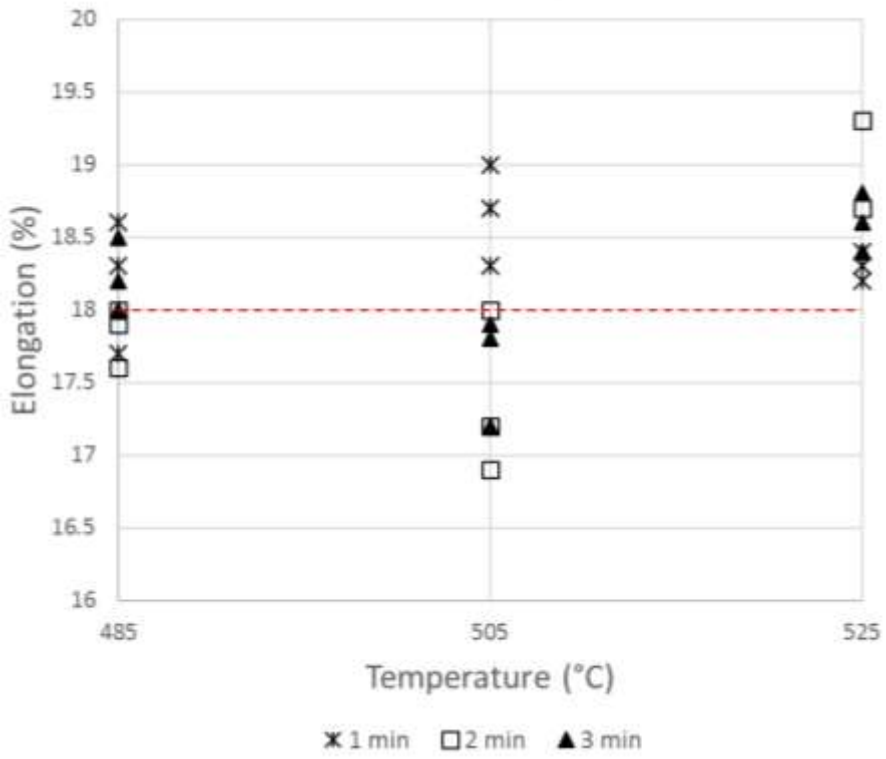

Figure 23: Elongation Individual Value Plot grouped into heat treatment parameters for samples heat treated in the sand bath. Dashed line refers to the average Elongation for the current HLT process.

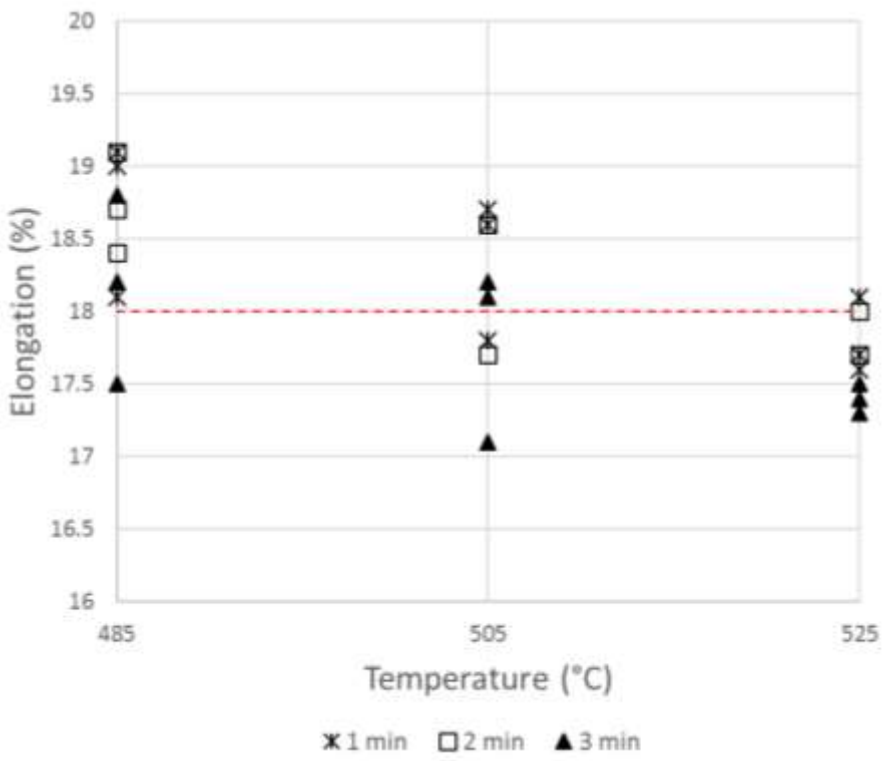

Figure 24: Elongation Individual Value Plot grouped into heat treatment parameters for samples heat treated in the salt bath. Dashed line refers to the average Elongation for the current HLT process.

The regression ANOVA analysis for the elongation showed the heat treatment equipment variable was not found to be statistically significant with a p-value of 0.556. Time and temperature also did not show statistical significance with p-values of 0.057 and 0.436, respectively. Temperature, heat treatment equipment and the temperature did not show statistical significance with p-values greater than 0.05. The elongation normal probability plot of residuals for 54 samples form a nearly linear pattern, which indicated that the normal distribution is a good model for the data set (Figure 25). However, the ANOVA model for a regression model of the elongation had a goodness of fit R-squared

values between 0.00% to 8.69%. These values span a range less than 10%, however the values are lower than 60% which results in a decrease in confidence in the elongation model for the data range observed. Temperature and the heat treatment equipment did not have a significant impact on the elongation percentage. It is difficult to determine exactly how elongation is impacted with the data available.

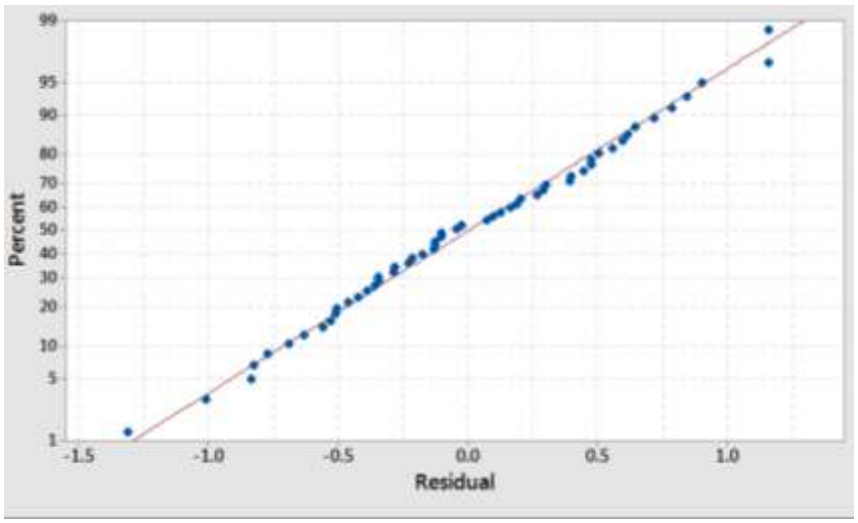

Figure 25: Elongation (%) Normal Probability Plot of Residuals

4.3.3 Strain-Based Mechanical Properties Summary

The strain-based mechanical properties were not easily modeled and therefore difficult to conclude trends that could be used to predict the residual elongation and elongation for future samples. Residual elongation data was much more highly variable than the stress-based mechanical properties. Skew left normal probability plot of residuals. The goodness of fit R-squared values ranged from 33.94% to 47.81%. The combination of the normal probability plot having a skew and the R-squared values not meeting the standard set results in a decrease in confidence in forming a linear model of the residual elongation that could predict the value of the residual elongation of future test samples.

Despite this, some general trends were observed in the data correlating residual elongation to the temperature and heat treatment equipment. Both variables yielded significant p-values, with the heat treatment equipment having the larger impact on residual elongation. The residual elongation did not show a statistical impact by changes in time. The difference in residual elongation for the heat treatment equipment is most evident by the data spread. The salt bath parts had very compact data that did not fluctuate much with time or temperature. The sand bath parts did not show a consistent trend across the input range. No obvious trends are observed in the data and therefore further investigation must be conducted before defining the impacts time, temperature and heat treatment equipment have on residual elongation. The elongation was difficult to model and therefore made the effect of time on elongation unclear even though the ANOVA test yielded a significant p-value less than 0.05. Goodness of fit R-squared values were extremely low for the elongation model. Temperature and heat treatment equipment did not have statistically significant p-values that would provide any evidence that temperature or heat treatment equipment impact elongation.

4.4 Summary of Samples Grouped via Heat Treatment Parameters

When the data is extrapolated within the test range contour plots for the sand bath and the salt bath are produced. Figure 26 and Figure 27 are the contour plots for the sand bath and salt bath, respectively. The white areas in the contour plots represent areas of acceptable combination of heat treatment parameters.

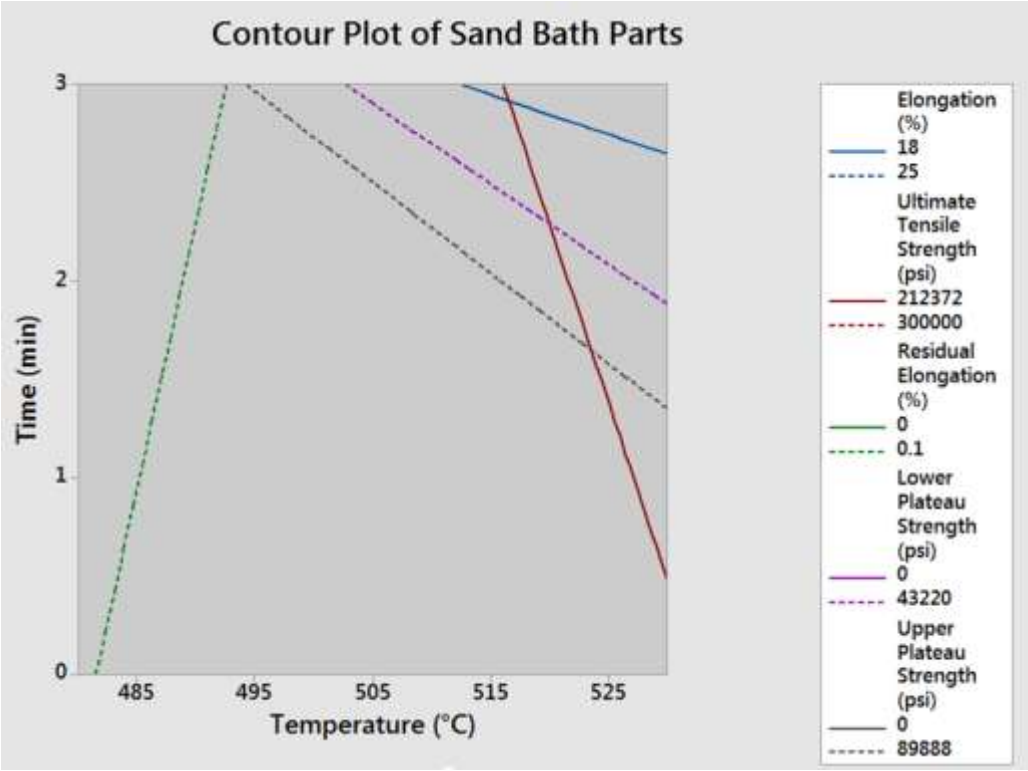

Figure 26: Contour Plot for acceptable sand bath parts (white area represents area of acceptable combination of heat treatment parameters)

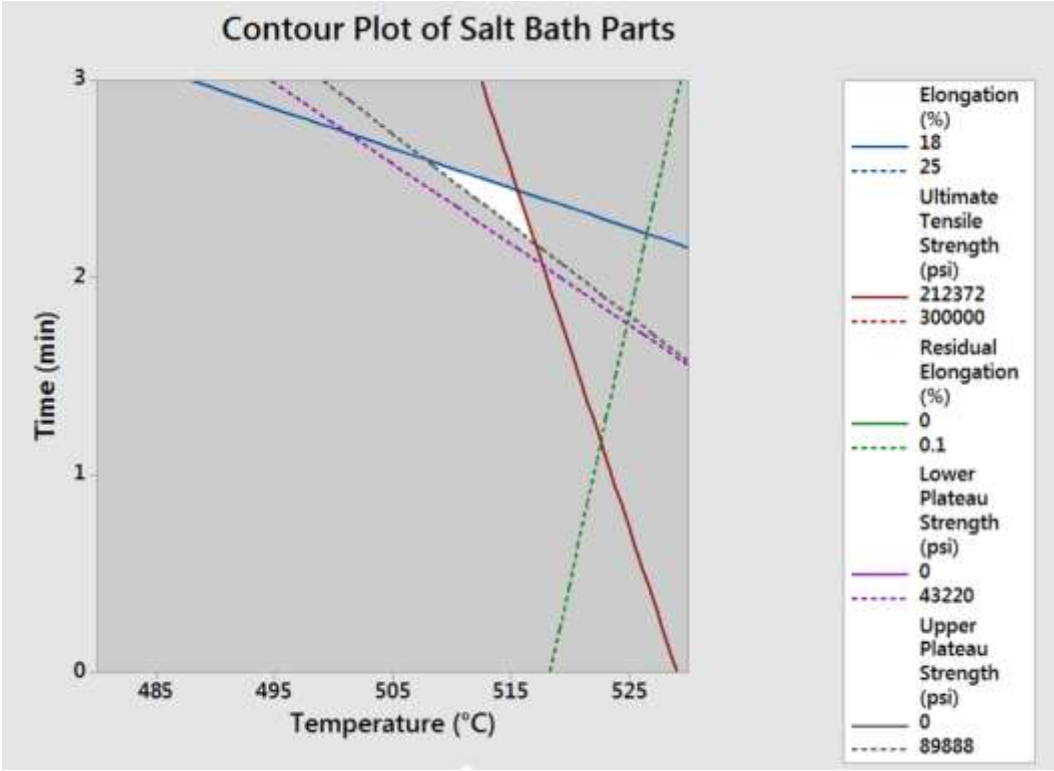

Figure 27: Contour Plot for acceptable salt bath parts

Analysis via Contour Plots show that there exists a design space for the salt bath, however there is no combination of sand bath parameters that results in the desired mechanical properties for the Nitinol wire. The space for the salt bath does not include any of the tested sample groups however 1 sample group (505°C Salt Bath 3 minutes) meets all requirements except for 1 sample within that group that does not meeting the Elongation requirement. A summary of that data is provided in Table 2.

Table 2: Process group closest to passing all mechanical property requirements

Description	Diameter (in)	Upper Plateau Strength (psi)	Lower Plateau Strength (psi)	Residual Elongation (%)	Ultimate Tensile Strength (psi)	Elongation (%)
Salt Bath 505°C 3 min	0.01116	88,250	41,218	0.09	219,988	18.2
	0.01116	88,411	41,242	0.06	219,639	17.1
	0.01116	88,312	40,762	0.07	219,614	18.1

4.5 Effect of A_f Temperature

To analyze the effect of transition temperatures, sample groups heat treated in the sand bath and salt bath were matched up based on A_f temperature. A_f temperature was determined using DSC. Raw data for DSC testing done by Legend Technical Services (St. Paul, MN) can be found in Appendix D and is plotted in Figure 28 and Figure 29.

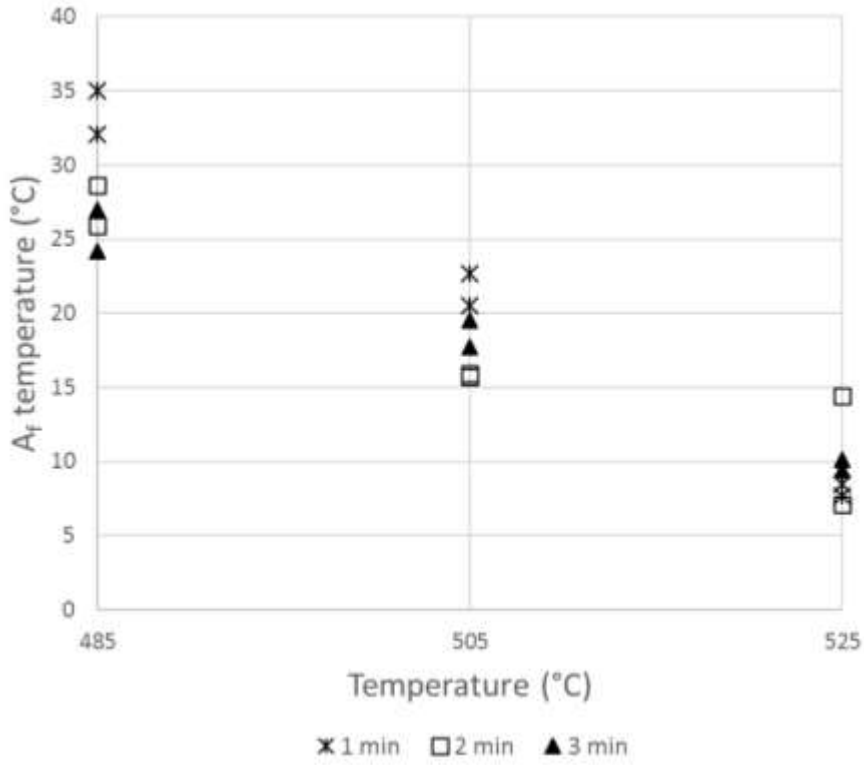

Figure 28: A_f temperature Value Plot grouped into heat treatment parameters for samples heat treated in the sand bath

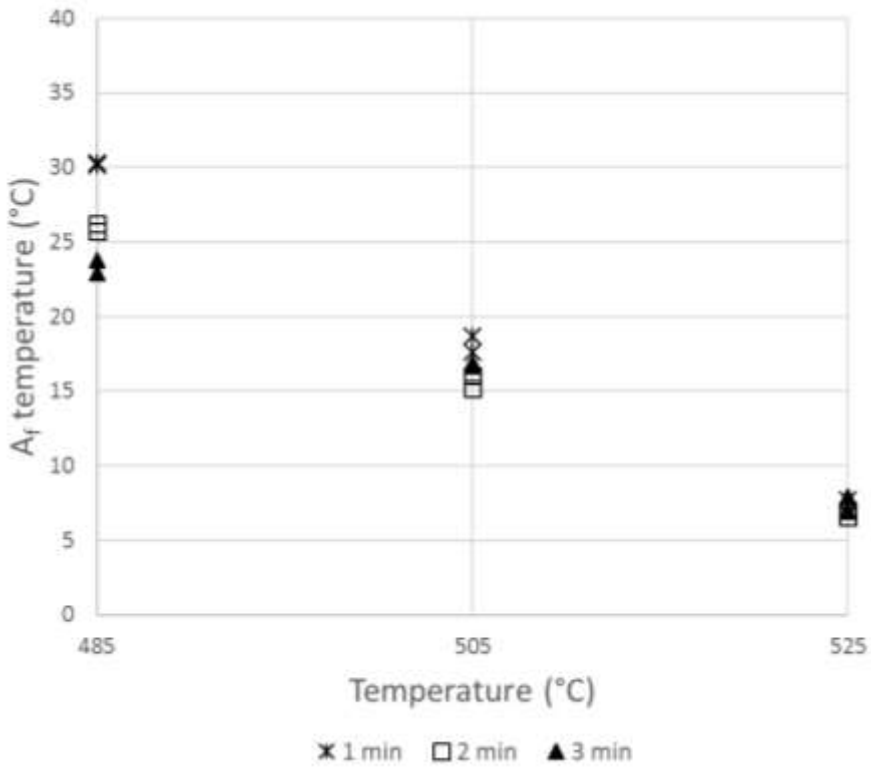

Figure 29: A_f temperature Value Plot grouped into heat treatment parameters for samples heat treated in the salt bath

For the purpose of studying the effect of A_f temperature, four sample groups were created by combining sand and salt heat treated samples that had similar values for A_f (Table 3). The DSC results from the same sample group were averaged and used as the A_f temperature for all samples in that group. A 0.5°C temperature difference was deemed equivalent for matching sand bath groups to salt bath groups.

Table 3: A_f sample groups

	Sand			Salt		
A_f group	Temp (°C)	Time (min)	Af temperature	Temp (°C)	Time (min)	Af temperature
1	525	1	8.1	525	3	8.25
2	505	2	15.8	505	2	15.6
3	505	3	18.6	505	1	18.15
4	485	3	25.6	485	2	25.95

A regression ANOVA test was conducted to compare the groups to see if the heat treatment equipment had a significant impact on mechanical performance when the A_f temperature is the same. Time and temperature input variables were not included in the model. When developing predictive models using A_f temperature as an input parameter in place of time and temperature, the only mechanical property that yielded a goodness of fit above 60% was ultimate tensile strength (76.44%). However, the heat treatment equipment does not yield a statistically significant different UTS when A_f temperature is considered for the study range.

The R-squared predictive value for upper plateau strength and lower plateau strength was 0.00%. The elongation model was not significantly greater having an R-squared predictive value below 1%. The R-squared predicted values for the residual elongation was 38.20%. These values are lower than 60% which results in a decrease in confidence in drawing conclusions from the residual elongation model for the data range observed. This is most likely from the limited data in this study, as previous studies have investigated A_f temperatures effect on the mechanical properties [13], [14]. A_f temperature had a significant impact on all tensile factors as expected. Assuming the ultimate tensile

strength was an acceptable model, it would remain unclear if the degradation caused by the heat treatment temperature had a significant impact [13], [14].

5 Conclusions and Future Work

Studies have been conducted comparing the effect of different Nitinol wire heat treatment methods/parameters or the effect of different Nitinol wire processing on tensile data. The effect of the heat treatment equipment has not been investigated in as much detail. The purpose of this study was to fill this gap in public information by analyzing the mechanical behavior differences between Nitinol wire heat treated in a salt bath and Nitinol wire heat treated in a sand bath. The first goal was to determine if the heat treatment methods result in significant differences in the mechanical properties: upper plateau strength, lower plateau strength, residual elongation, ultimate tensile strength, and elongation.

Tensile results were obtained for eighteen sample groups with three replicates for each group. An ANOVA analysis was conducted showing that the heat treatment temperature and A_f temperature had a significant impact on all tensile factors as expected. When considering the effect of the heat treatment equipment, the regression model analyses showed that the heat treatment equipment had a statistically significant impact on lower plateau strength, residual elongation and ultimate tensile strength, but did not show a statistically significant impact on the upper plateau strength or elongation. It should be noted that the residual elongation model was not statistically accurate enough to give confidence in predicting future samples based on the data gathered in this study.

The available data and knowledge collected from this study show that the salt bath would be the recommended equipment due to the benefits of a faster ramp up and more

consistent temperature seen in the temperature traces and the more repeatable mechanical performance within sample groups.

To improve on the existing process at HLT Inc., a switch from the sand bath to the salt bath is recommended. This change gives an improved design space to obtain the desired mechanical properties of the wire. In addition, the tensile measurements are more repeatable when comparing sand bath sample groups with salt bath sample groups. A range finding study should be conducted with more sample groups selected within and around the salt bath contour plot design area seen in Figure 27. This testing will more accurately map the process parameters before the necessary valve tests are performed and the final time and temperature parameters are determined.

Samples grouped based on A_f temperature did not have different heat treatment temperatures. Therefore, the analysis should show the correlation between A_f temperature and the mechanical properties is similar or linked to the correlation between temperature and the mechanical properties. To evaluate the effect A_f temperature has on the mechanical properties independent from the effect of temperature, more samples will need to be made that have the same A_f temperature processed at different heat treatment temperatures. This would most likely be accomplished by heat treating parts at the high temperatures for a longer time.

Further experiments should be performed to include additional input variables and their effect on the mechanical properties. The missing factor(s) for predictive models could include the size, density and/or location of inclusions in the wire, grain microstructure and material phase orientation along the wire sample or a change in the tensile test set-up from

sample to sample that was uncaptured/unobserved at the time of testing. It is also possible that a different form of equation, besides linear, gives a better fit for the predictive model. There could also capture variable interactions that weren't captured in this testing/analysis. A higher quantity of samples per sample group could also reduce the current sample variation/spread seen in the current data set and give more confidence in the stress and strain predictive models.

The missing factor(s) for predictive models for residual elongation and elongation could include the inclusion size, inclusion density and/or location of inclusions in the wire, grain microstructure, changes in cold work and material phase orientation along the wire sample or a change in the tensile test set-up from sample to sample that was uncaptured/unobserved at the time of testing. All these factors were attempted to be held constant by the controls put in place: all samples were taken from the same lot of wire; all samples were wrapped, and heat treated by one person and all tensile testing was conducted by Fort Wayne. It is also possible that a different form of equation beyond linear is possible to capture a better fit. There could also be a variable interaction involved. A higher quantity of samples per sample group could also help account for the larger variation/spread seen in the strain (residual elongation and elongation) individual value plots when compared to the stress (upper plateau strength, lower plateau strength, ultimate tensile strength) individual value plots.

6 Bibliography

[1] Graff, L. (2018). How It Works – Developing a Good Memory: Nitinol Shape Memory Alloy. *Today's Machining World*. Retrieved from todaysmachiningworld.com/magazine/how-it-works-developing-a-good-memorynitinol-shape-memory-alloy/.

[2] (2007). Nitinol Shape Memory Alloy Introduction. History of Nitinol, Images Scientific Instruments. Retrieved from www.imagesco.com/articles/nitinol/01.html.

[3] Kauffman, G. B., & Mayo, I. (1997). The story of nitinol: the serendipitous discovery of the memory metal and its applications. *The chemical educator*, *2*(2), 1-21.

[4] Ackland, G. J., & Pinsook, U. (2002). How Do Martensitic Twin Boundaries Move?. *MRS Online Proceedings Library Archive*, *731*.

[5] Chekotu, J. C., Groarke, R., O'Toole, K., & Brabazon, D. (2019). Advances in selective laser melting of nitinol shape memory alloy part production. *Materials*, *12*(5), 809.

[6] Wayman, C. M. (1994). About Shape Memory Alloys. In *Superconductors, Surfaces and Superlattices* (pp. 973-998). Elsevier.

[7] Kowalczyk, M., & Niżankowski, C. (2017). Comparative analysis of machinability of nitinol alloy using weighted radar diagram. *Management and Production Engineering Review*, *8*.

[8] Stöckel, D. (1995). The shape memory effect-phenomenon, alloys and applications. *Proceedings: Shape Memory Alloys for Power Systems EPRI*, *1*, 1-13.

[9] Gallardo Fuentes, J. M., Gümpel, P., & Strittmatter, J. (2002). Phase change behavior of nitinol shape memory alloys. *Advanced engineering materials*, *4*(7), 437-452.

[10] Duerig, T. W., & Zadno, R. (1990). An engineer's perspective of pseudoelasticity. *Engineering aspects of shape memory alloys*, 369-393.

[11] Pelton, A. R., Russell, S. M., & DiCello, J. (2003). The physical metallurgy of nitinol for medical applications. *Jom*, *55*(5), 33-37.

[12] Nitinol - Frequently Asked Questions. *Smart Wires*. Retrieved from smartwires.eu/index.php?id_cms=9&controller=cms&id_lang=1.

[13] Pelton, A. R., Dicello, J., & Miyazaki, S. (2000). Optimization of processing and properties of medical grade Nitinol wire. *Minimally Invasive Therapy & Allied Technologies*, *9*(2), 107-118.

[14] Drexel, M., Selvaduray, G., & Pelton, A. (2007). The Effects of Cold Work and Heat Treatment on the Properties of Nitinol Wire (Vol. 42665, pp. 89-90).

[15] ASTM. (2017). ASTM F2004-17 Standard Test Method for Transformation Temperature of Nickel-Titanium Alloys by Thermal Analysis. ASTM International. West Conshohocken, PA.

[16] ASTM. (2016). ASTM F2082 / F2082M-16, Standard Test Method for Determination of Transformation Temperature of Nickel-Titanium Shape Memory Alloys by Bend and Free Recovery. ASTM International. West Conshohocken, PA.

[17] ASTM. (2014). ASTM F2516-14, Standard Test Method for Tension Testing of Nickel-Titanium Superelastic Materials. ASTM International. West Conshohocken, PA.

[18] Kapoor, D. (2017). Nitinol Parts for Stents | Nickel Titanium Shape Memory Alloys". Johnson Matthey Technology Review. Retrieved from www.technology.matthey.com/article/61/1/66-76/

[19] (2018). Measuring Transformation Temperatures in Nitinol Alloys". Setting Shapes in Nitinol: Niti Superelasticity and Shape Memory Properties. Retrieved from jmmedical.com/resources/211/Measuring-Transformation-Temperatures-in-Nitinol-Alloys.html.

[20] Burns, G. W., & Scroger, M. G. (1989). *The calibration of thermocouples and thermocouple materials* (Vol. 250, No. 35). US Department of Commerce, National Institute of Standards and Technology.

[21] Morgan, N. (2018). Introduction to Nitinol. SMST Conference, Galway, Ireland.

Appendix A: Sand and Salt Bath Traces

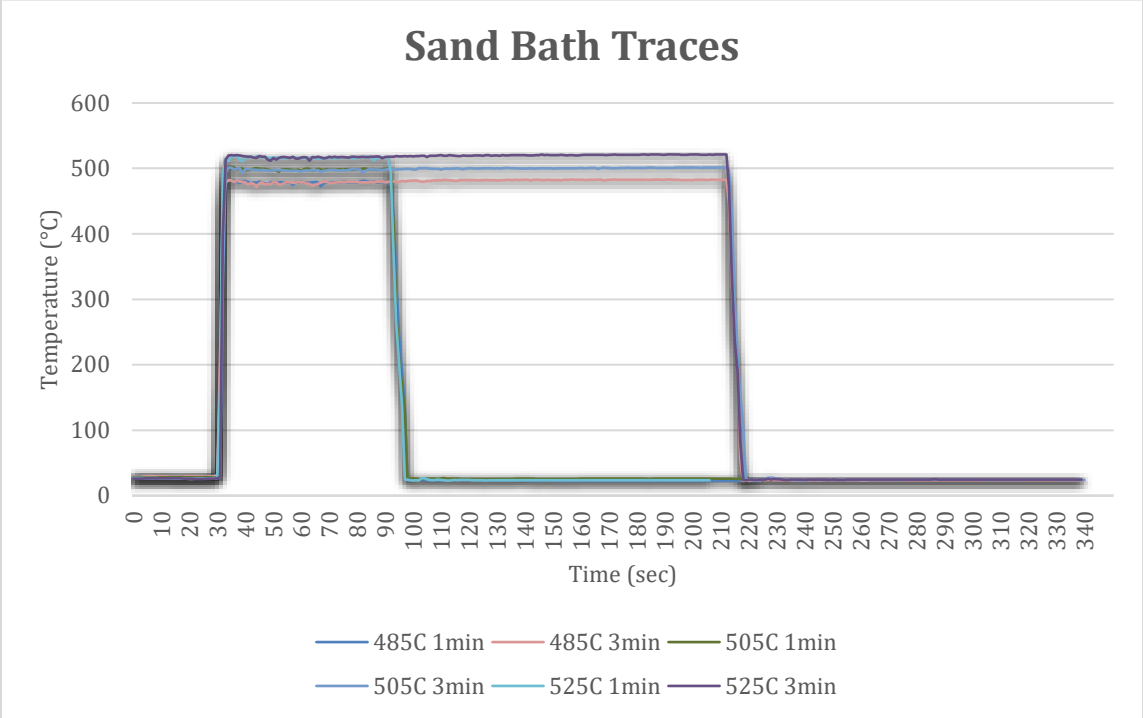

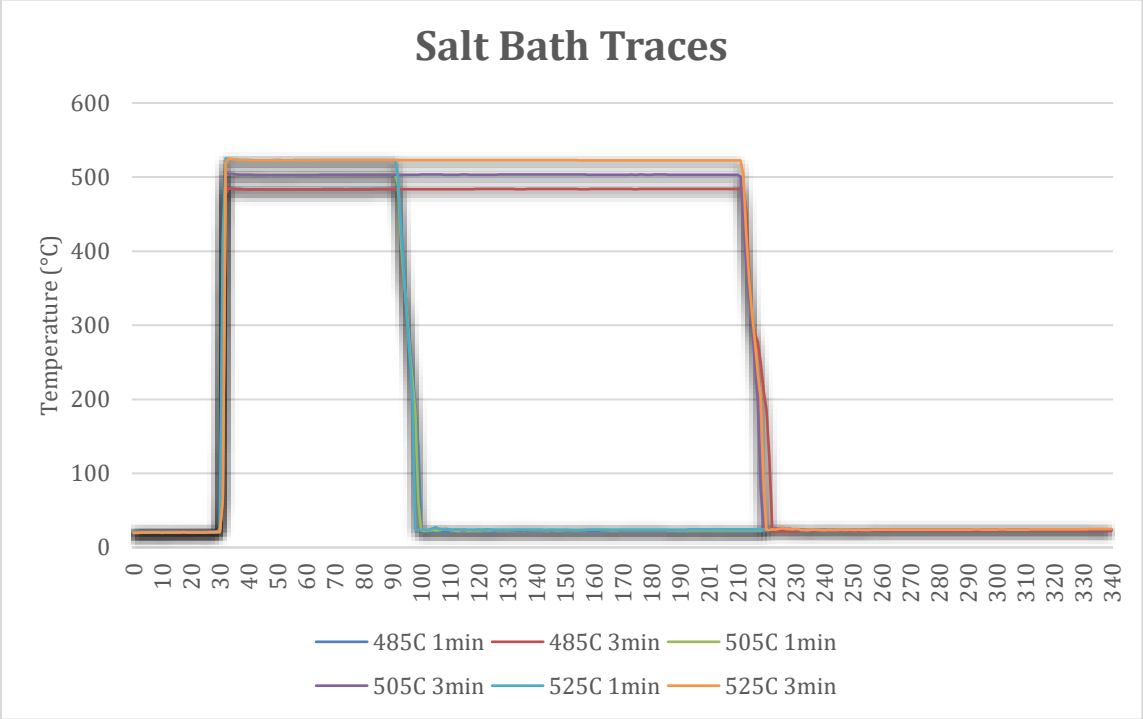

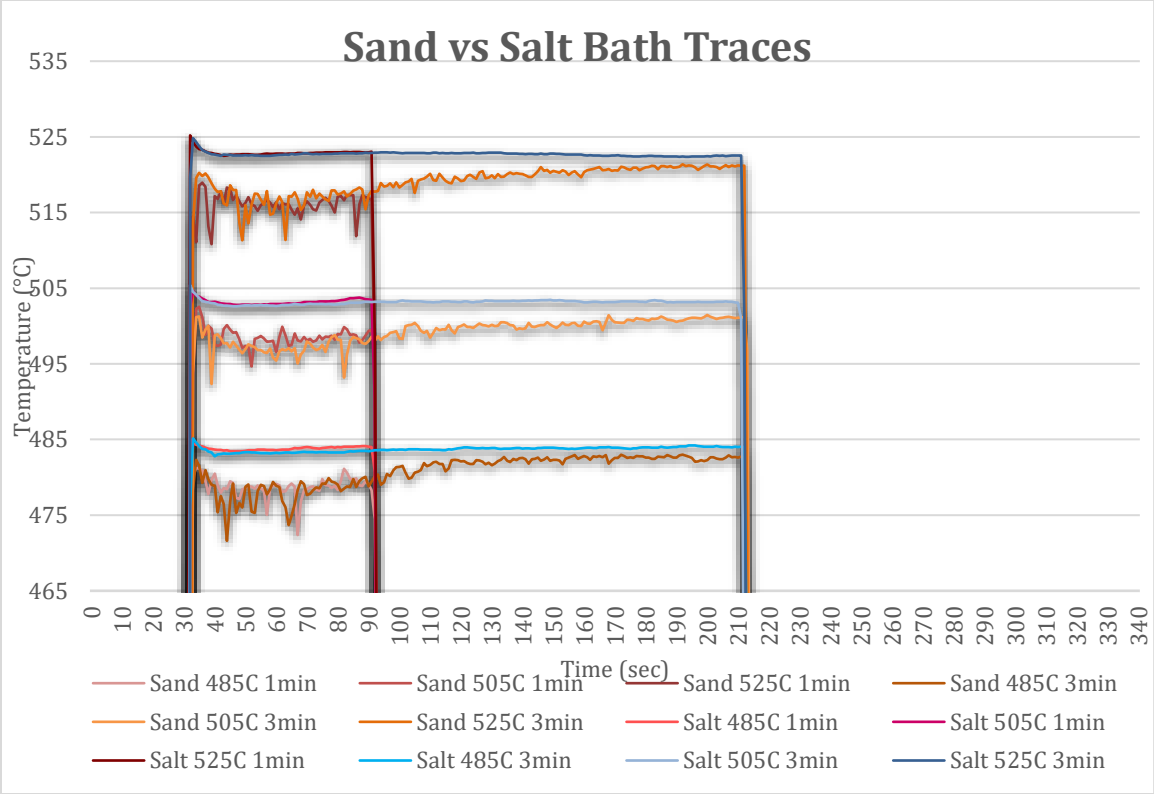
Sand vs Salt Bath Traces
535
525
515
505
495
485
475
465
Temperature (°C)
0
10
20
30
40
50
60
70
80
90
100
110
120
130
140
150
160
170
180
190
200
210
220
230
240
250
260
270
280
290
300
310
320
330
340
Time (sec)
Sand 485C 1min
Sand 505C 1min
Sand 525C 1min
Sand 485C 3min
Sand 505C 3min
Sand 525C 3min
Salt 485C 1min
Salt 505C 1min
Salt 525C 1min
Salt 485C 3min
Salt 505C 3min
Salt 525C 3min

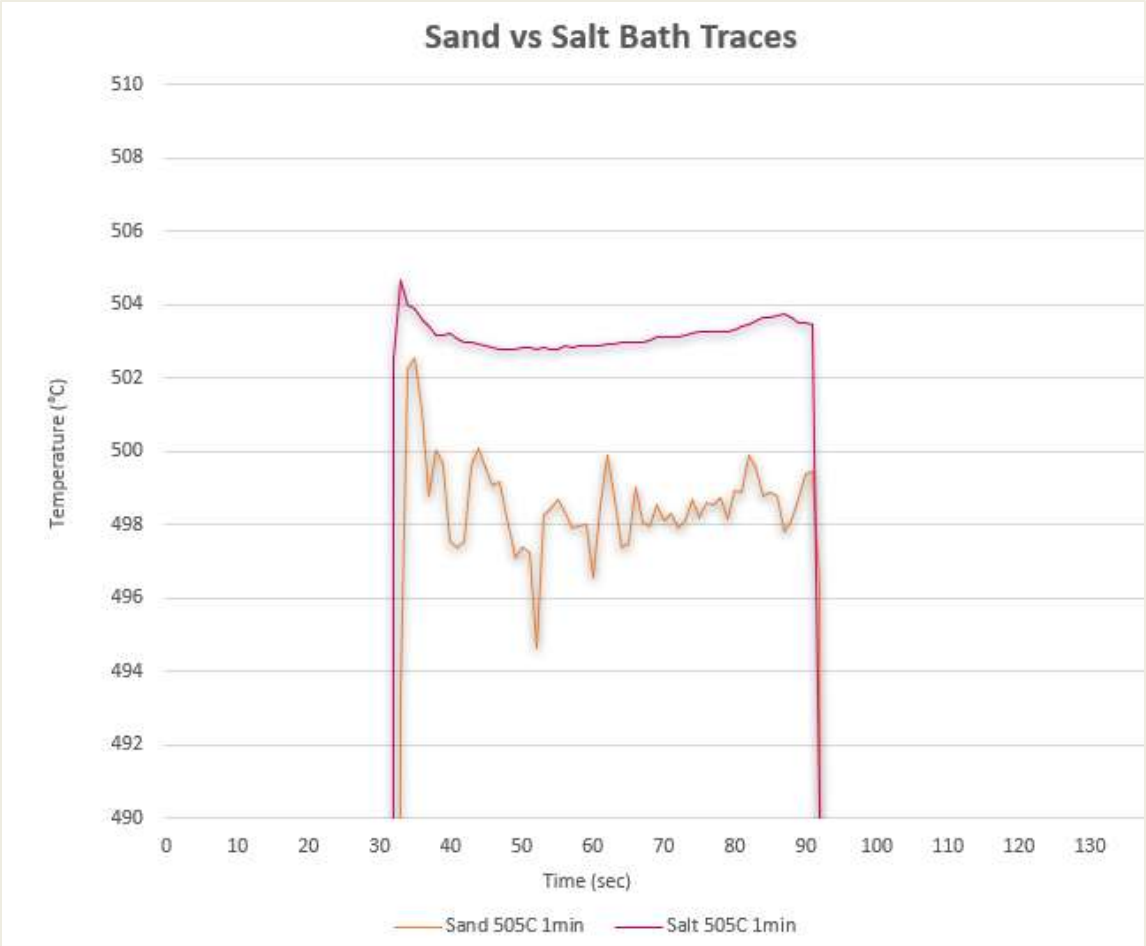
Sand vs Salt Bath Traces
510
508
506
504
502
500
498
496
494
492
490
Temperature (°C)
0
10
20
30
40
50
60
70
80
90
100
110
120
130
Time (sec)
Sand 505C 1min
Salt 505C 1min

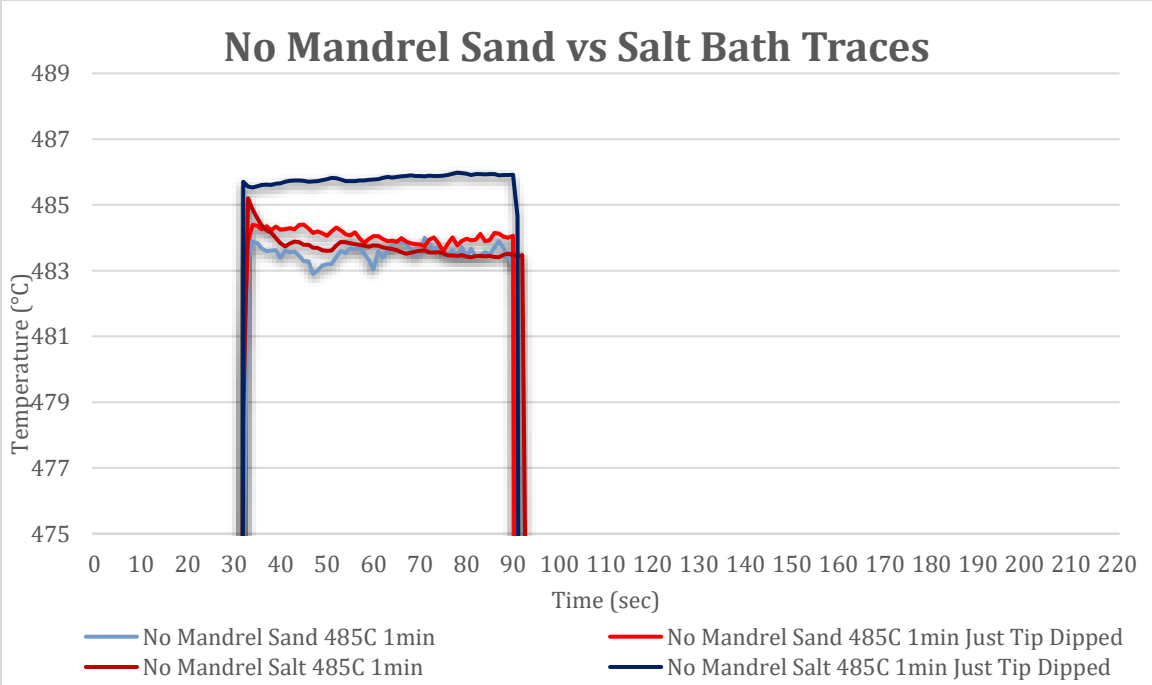
No Mandrel Sand vs Salt Bath Traces
489
487
485
483
481
479
477
475
Temperature (°C)
0 10 20 30 40 50 60 70 80 90 100 110 120 130 140 150 160 170 180 190 200 210 220
Time (sec)
No Mandrel Sand 485C 1min
No Mandrel Sand 485C 1min Just Tip Dipped
No Mandrel Salt 485C 1min
No Mandrel Salt 485C 1min Just Tip Dipped

Appendix B: Sand Bath Tensile Data

Description	Diameter (in)	Upper Plateau Strength (psi)	Lower Plateau Strength (psi)	Residual Elongation (%)	Ultimate Tensile Strength (psi)	Elongation (%)
525° Sand Bath 1min Water 2min	0.01122	91,588	51,103	0.24	212,901	18.3
	0.01122	92,333	46,903	0.14	215,052	18.4
	0.01114	93,689	47,429	0.13	215,599	18.2
525° Sand Bath 2min Water 2min	0.01118	87,881	42,064	0.20	209,150	18.7
	0.01122	87,216	41,251	0.20	207,184	19.3
	0.01122	89,084	42,753	0.12	208,618	19.3
525° Sand Bath 3min Water 2min	0.01116	85,496	37,800	0.12	204,408	18.8
	0.01116	86,536	38,047	0.08	206,118	18.6
	0.01116	86,915	38,199	0.17	205,960	18.4
505° Sand Bath 1min Water 2min	0.01118	90,257	54,176	0.09	229,120	18.3
	0.01118	95,433	49,862	0.08	230,219	18.7
	0.01118	90,103	53,583	0.11	229,383	19.0
505° Sand Bath 2min Water 2min	0.01116	88,988	51,384	0.21	223,767	18.0
	0.01116	92,244	45,744	0.09	223,816	17.2
	0.01118	91,926	45,477	0.08	222,589	16.9
505° Sand Bath 3min Water 2min	0.01116	85,369	47,594	0.16	222,075	17.8
	0.01116	89,720	41,996	0.07	222,147	17.9
	0.01116	89,923	41,931	0.08	221,943	17.2
485° Sand Bath 1min Water 2mi	0.01118	95,939	50,864	0.09	239,725	18.6
	0.01118	95,080	51,319	0.07	239,109	18.3
	0.01118	95,604	51,151	0.09	239,392	17.7
485° Sand Bath 2min Water 2min	0.01116	95,552	49,527	0.07	236,755	18.0
	0.01116	90,086	52,804	0.12	234,283	17.6
	0.01116	94,575	48,907	0.06	234,749	17.9
485° Sand Bath 3min Water 2min	0.01116	92,352	46,541	0.14	232,577	18.0
	0.01116	92,975	47,003	0.08	234,883	18.5
	0.01116	92,494	46,638	0.07	232,194	18.2

Appendix C: Salt Bath Tensile Data

Description	Diameter (in)	Upper Plateau Strength (psi)	Lower Plateau Strength (psi)	Residual Elongation (%)	Ultimate Tensile Strength (psi)	Elongation (%)
525° Salt Bath 1min Water 2min	0.01118	91,811	47,293	0.08	211,018	17.7
	0.01118	92,391	47,704	0.08	211,291	17.6
	0.01118	92,935	47,701	0.10	211,356	18.1
525° Salt Bath 2min Water 2min	0.01116	88,474	41,733	0.08	206,707	17.7
	0.01116	89,061	42,570	0.09	206,122	18.0
	0.01116	89,752	43,098	0.09	206,627	17.7
525° Salt Bath 3min Water 2min	0.01116	85,794	37,645	0.08	202,215	17.3
	0.01116	85,978	37,395	0.10	202,095	17.4
	0.01116	87,147	37,748	0.08	203,720	17.5
505° Salt Bath 1min Water 2min	0.01116	93,820	48,826	0.09	226,553	18.6
	0.01116	94,814	48,954	0.09	225,964	18.7
	0.01116	94,595	49,369	0.06	227,386	17.8
505° Salt Bath 2min Water 2min	0.01116	93,206	45,568	0.11	222,040	18.6
	0.01116	91,774	44,858	0.06	221,598	17.7
	0.01116	92,932	45,314	0.07	221,964	18.6
505° Salt Bath 3min Water 2min	0.01116	88,250	41,218	0.09	219,988	18.2
	0.01116	88,411	41,242	0.06	219,639	17.1
	0.01116	88,312	40,762	0.07	219,614	18.1
485° Salt Bath 1min Water 2min	0.01116	95,195	50,054	0.09	236,334	19.0
	0.01116	95,471	50,479	0.08	237,505	19.1
	0.01116	94,724	49,892	0.07	236,612	18.1
485° Salt Bath 2min Water 2min	0.01116	93,587	48,046	0.07	233,306	18.4
	0.01116	94,218	48,454	0.07	233,615	19.1
	0.01116	90,346	52,805	0.06	232,889	18.7
485° Salt Bath 3min Water 2min	0.01116	92,355	45,961	0.07	231,252	18.2
	0.01116	92,962	45,948	0.06	230,290	17.5
	0.01116	92,317	45,891	0.06	230,739	18.8

Appendix D: DSC Testing Raw Data Results

Heat Treatment Equipment	Heat Treatment Temperature (°C)	Heat Treatment Time (min)	A_f temperature (°C)	Average A_f temperature (°C)
Sand Bath	485	1	32.1	33.55
			35.0	
		2	25.9	27.25
			28.6	
		3	27.0	25.6
			24.2	
	505	1	20.5	21.6
			22.7	
		2	15.9	15.8
			15.7	
		3	19.5	18.6
			17.7	
	525	1	8.5	8.1
			7.7	
		2	7.1	10.75
			14.4	
		3	10.1	9.75
			9.4	
Salt Bath	485	1	30.3	30.25
			30.2	
		2	26.2	25.95
			25.7	
		3	22.9	23.35
			23.8	
	505	1	18.7	18.15
			17.6	
		2	16.0	15.6
			15.2	
		3	16.8	16.75
			16.7	
	525	1	7.7	7.3
			6.9	
		2	6.6	6.8
			7.0	
		3	7.9	8.25
			8.6	